

See discussions, stats, and author profiles for this publication at: <https://www.researchgate.net/publication/47659537>

# Vibrational Analysis of Amino Acids and Short Peptides in Hydrated Media. VIII. Amino Acids with Aromatic Side Chains: L-Phenylalanine, L-Tyrosine, and L-Tryptophan

ARTICLE *in* THE JOURNAL OF PHYSICAL CHEMISTRY B · NOVEMBER 2010

Impact Factor: 3.3 · DOI: 10.1021/jp106786j · Source: PubMed

---

CITATIONS

31

READS

47

## 5 AUTHORS, INCLUDING:



[Belen Hernández](#)

Université Paris 13 Nord

39 PUBLICATIONS 369 CITATIONS

[SEE PROFILE](#)



[Fernando Pfluger](#)

Université Paris 13 Nord

23 PUBLICATIONS 323 CITATIONS

[SEE PROFILE](#)



[Sergei G Kruglik](#)

Pierre and Marie Curie University - Paris 6

99 PUBLICATIONS 904 CITATIONS

[SEE PROFILE](#)



[Mahmoud Ghomi](#)

Université Paris 13 Nord

112 PUBLICATIONS 1,753 CITATIONS

[SEE PROFILE](#)

# Vibrational Analysis of Amino Acids and Short Peptides in Hydrated Media. VIII. Amino Acids with Aromatic Side Chains: L-Phenylalanine, L-Tyrosine, and L-Tryptophan

Bélén Hernández,<sup>†</sup> Fernando Pflüger,<sup>†</sup> Alain Adenier,<sup>‡</sup> Sergei G. Kruglik,<sup>§</sup> and Mahmoud Ghomi\*,<sup>†</sup>

*Groupe de Biophysique Moléculaire, UFR SMBH, Université Paris 13, 74 rue Marcel Cachin, 93017 Bobigny cedex, France; Laboratoire ITODYS, UMR 7086, Université Paris Diderot, Bâtiment Lavoisier, 15, rue Jean-Antoine de Baïf, 75205 Paris cedex 13, France; and Laboratoire Acides Nucléiques et Biophotonique (FRE 3207), Université Pierre et Marie Curie Paris 06, 75252 Paris, France*

Received: July 21, 2010; Revised Manuscript Received: October 4, 2010

Four out of the 20 natural  $\alpha$ -amino acids ( $\alpha$ -AAs) contain aromatic rings in their side chains. In a recent paper (*J. Phys. Chem. B* 2010, 114, 9072–9083), we have analyzed the structural and vibrational features of L-histidine, one of the potent elements of this series. Here, we report on the three remaining members of this family, i.e., L-phenylalanine, L-tyrosine, and L-tryptophan. Their solution ( $H_2O$  and  $D_2O$ ) Raman scattering and Fourier transform infrared absorption attenuated total reflection (FT-IR ATR) spectra were measured at room temperature from the species corresponding to those existing at physiological conditions. Because of the very low water solubility of tyrosine, special attention was paid to avoid any artifact concerning the report of the vibrational spectra corresponding to nondissolved powder of this AA in aqueous solution. Finally, we could obtain for the first time the Raman and FT-IR spectra of tyrosine at very low concentration (2.3 mM) upon long accumulation time. To clarify this point, those vibrational spectra of tyrosine recorded either in the solid phase or in a heterogeneous state, where dissolved and nondissolved species of this AA coexist in aqueous solution, are also provided as Supporting Information. To carry out a discussion on the general geometrical and vibrational behavior of these AAs, we resorted to quantum mechanical calculations at the DFT/B3LYP/6-31++G\* level, allowing (i) determination of potential energy surfaces of these AAs in a continuum solvent as a function of the torsion angles  $\chi_1$  and  $\chi_2$ , defining the conformation of each aromatic side chain around  $C_\alpha-C_\beta$  and  $C_\beta-C_\gamma$  bonds, respectively; (ii) analysis of geometrical features of the AAs surrounded by clusters of  $n$  explicit ( $n = 5–7$ ) water molecules interacting with the backbone and aromatic rings; and (iii) assignment of the observed vibrational modes by means of the theoretical data provided by the lowest energy conformers of explicitly hydrated amino acids.

## I. Introduction

L-phenylalanine (Phe or F) and L-tryptophan (Trp or W) belong to the family of essential  $\alpha$ -amino acids ( $\alpha$ -AAs) and cannot be synthesized by the human organism, whereas L-tyrosine (Tyr or Y) can be classified among the conditionally essential AAs.<sup>1–3</sup>

The common structural feature of these three natural AAs is an aromatic ring connected to the  $C_\beta$  atom of their side chains (Figure 1).<sup>4</sup> Phe, the structurally simplest AA of this group, contains a phenyl ring in its side chain. Tyr is synthesized in the body from Phe under the action of a hepatic enzyme, phenylalanine hydroxylase (PAH), responsible for the phenyl-to-phenol ring conversion of the side chain. The PAH deficiency leads to Phe accumulation, which is converted into phenylketone, leading to a metabolic disorder named phenylketonuria (PKU).<sup>5,6</sup> In this case, Tyr becomes an essential amino acid and should be provided to the organism. Tyr is considered as a biochemical precursor of many other biologically important molecules, such as dihydroxyphenylalanine (DOPA), adrenalin, dopamin, and melanin.<sup>7,8</sup> On the other hand, the presence of

the hydroxyl function allows phosphorylation of tyrosine side chain by the intermediate of kinases, a chemical transformation necessary for enzymatic regulation.<sup>9</sup> Topoisomerase I, the enzyme which can relax a stressed supercoiled DNA, cuts one of the DNA double helix strands through the formation of a reversible phosphotyrosine bond between a tyrosine hydroxyl group and a DNA phosphate group.<sup>10</sup> Trp, having an indole ring, a larger size side chain compared to the other two AAs (Figure 1), is also considered as a potent biochemical precursor, taking part in the synthesis of serotonin, niacin, and auxin.<sup>11–14</sup> In a peptide chain, the AAs with aromatic side chains are considered as potential recognition sites for certain enzymes. For instance, the C-terminal side of Phe, Tyr, and Trp (together with that of Leu and Met) residues serves as cleavage site for the enzyme chymotrypsin.<sup>15,16</sup>

These AAs also play a pivotal role in the physical properties of peptides and proteins. (i) Because their side-chain rings can be stacked one with another, and Tyr and Trp rings can take part in H-bond interactions (through their OH and NH groups, respectively), these AAs contribute to the structural stabilization and self-assembly of short peptides,<sup>17,18</sup> soluble,<sup>19</sup> and transmembrane<sup>20</sup> proteins. (ii) In relation to their ground → excited electronic transitions, *fluorescence effect*, consisting of a UV light absorption followed by a delayed lower energy UV light emission, is considered as the common physical property of all

\* To whom correspondence should be addressed. E-mail: mahmoud.ghomi@univ-paris13.fr.

<sup>†</sup> Université Paris 13.

<sup>‡</sup> Université Paris Diderot.

<sup>§</sup> Université Pierre et Marie Curie Paris 06.

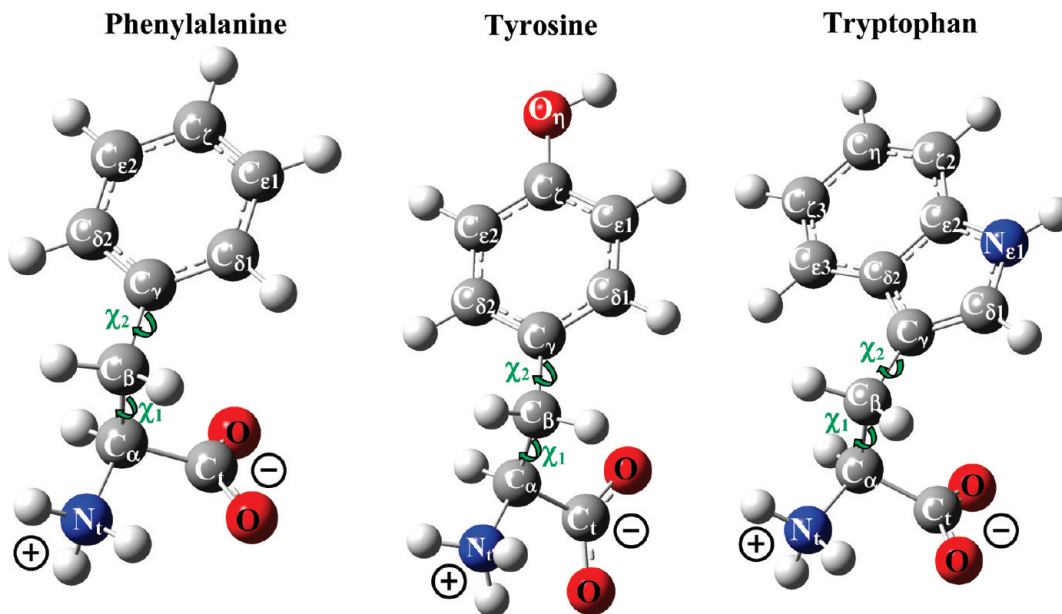


**Figure 1.** Zwitterionic forms of phenylalanine, tyrosine, and tryptophan. The side-chain conformation of these AAs can be defined by means of  $\chi_1$  and  $\chi_2$  torsion angles, with  $\chi_1 = \varphi(N_t-C_\alpha-C_\beta-C_\gamma)$  and  $\chi_2 = \varphi(C_\alpha-C_\beta-C_\gamma-C_\delta)$ . Note that in Phe,  $C_{\delta 1}$  and  $C_{\delta 2}$  atoms are equivalent. Consequently, there are two equivalent ways of defining  $\chi_2$  torsion angle. Thus, when one of the two values of  $\chi_2$  angle is given, the other one can be deduced upon addition of  $180^\circ$ .

these AAs.<sup>21</sup> However, the two main fluorescence factors, i.e., absorptivity and quantum yield, increase considerably in the order Phe  $\rightarrow$  Tyr  $\rightarrow$  Trp. As a consequence, when a peptide or a protein contains these three AAs, the resonance energy transfer from Phe to Tyr, and from Tyr to Trp, leads to the obtention of a fluorescence spectrum, resembling that of a Trp. Fluorescence spectra arising from these AAs have been used during the past years in the development of sensitive techniques,<sup>22</sup> allowing collection of information on the structural and dynamical properties of peptides and proteins, as well as on the metabolism of cells and tissues.<sup>23–25</sup> (iii) Phenyl, phenol, and indole rings give rise to a number of sharp Raman bands, characteristic of these  $\pi$ -conjugated systems,<sup>26,28,27</sup> known as environment-sensitive vibrational markers.

As already mentioned in the papers of this series devoted to amino acids,<sup>29–32</sup> our objective is to provide a set of comprehensive experimental and theoretical data on the vibrational analysis of the building blocks of peptides and proteins. In this framework, we have described an efficient protocol based on the joint use of aqueous solution ( $H_2O$  and  $D_2O$ ) vibrational spectra and quantum mechanical calculations in hydrated media, which was successfully applied to eight  $\alpha$ -AAs, i.e., Gly,<sup>29</sup> Ala,<sup>30</sup> Val,<sup>30</sup> Ile,<sup>30</sup> Leu,<sup>29,30</sup> Lys,<sup>31</sup> Arg,<sup>31</sup> and His.<sup>32</sup> To understand better the objective of the present report, we emphasize first the existing literature background available on the presently analyzed AAs, such as (i) IR spectra of the aromatic AAs recorded in  $H_2O$ ,<sup>33</sup> (ii) their surface-enhanced Raman spectra (SERS) on an electrochemically prepared silver surface,<sup>34</sup> (iii) self-consistent field (SCF) and density functional theory (DFT) calculations on isolated Phe,<sup>35,36</sup> (iv) ab initio molecular dynamics calculations of Phe +  $nH_2O$  clusters ( $n = 0–3$ ) with neutral and zwitterionic backbones,<sup>37</sup> (v) SCF<sup>38</sup> and DFT<sup>39</sup> calculations on isolated nonzwitterionic Tyr, (iv) photophysical properties of neutral and zwitterionic Tyr and Trp interacting with two water molecules as analyzed by theoretical calculations,<sup>40</sup> and (vi) hydration analysis of protonated aromatic AAs by the joint use of mass spectrometry, molecular mechanics, and quantum mechanical calculations.<sup>41</sup>

As it will be described, the aim of the present report is to improve first the existing data, to bring new data when it is lacking, and to discuss as adequately as possible the geometrical and vibrational features of the amino acids with aromatic side chains on the basis of new and unpublished theoretical data performed in a hydrated environment.

## II. Materials and Methods

**II.1. Experimental Section.** Lyophilized powders of L-phenylalanine (Merck), L-tyrosine, and L-tryptophan (Sigma-Aldrich) were dissolved either in water taken from a Millipore filtration system or in  $D_2O$  (100% purity) provided by Eurisotop (Saclay, France).  $D_2O/H_2O$  exchange was avoided by preparing deuterated samples under dry air atmosphere. The pH of prepared solutions was estimated with an accuracy of ca.  $\pm 0.1$ . Water solubility of these AAs at 25 °C rapidly decreases in the order Phe  $\rightarrow$  Trp  $\rightarrow$  Tyr, quantified by the values of 29.6, 11.4, and 0.45 mg/mL corresponding to Phe, Trp, and Tyr, respectively. In other words, the saturated molar concentrations are 182, 56, and 2.5 mM for Phe, Trp, and Tyr, respectively. Consequently, for Raman and IR measurements of the most soluble of these aromatic AAs (Phe and Trp), 50 mM solutions were used, i.e. just below the Trp limit concentration. This choice permitted obtention of intense and well resolved vibrational spectra for both AAs. In contrast, in the case of Tyr, after several attempts (see section III.1 for more details), we have finally used 2.3 mM (0.42 mg/mL) solutions, i.e. a concentration located just below the threshold of its solubility. It is to be stressed here that it is really a difficult task to record Tyr vibrational spectra at this low concentration. However, the signal/noise ratio could be improved by increasing the accumulation time, i.e., 60 scans of 50 s each for Tyr, and 40 scans of 30 s each for Phe and Trp. pH values of the three AAs, measured just after solution preparation, were 5.6 (Phe), 6.2 (Trp), and 6.4 (Tyr), i.e., those related to the neutral molecular species, all characterized by a zwitterionic backbone (Figure 1).

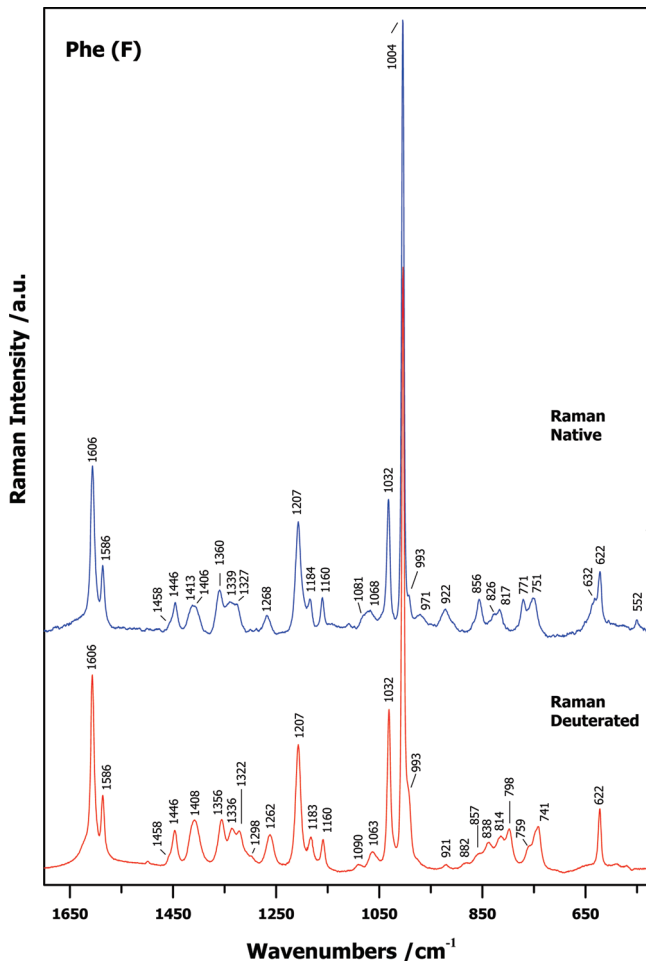


**Figure 2.** Room temperature Raman spectra ( $\lambda_L = 488$  nm) of phenylalanine observed in aqueous solutions: top,  $H_2O$  solution; bottom,  $D_2O$  solution. The intensity of each spectrum was normalized to its most intense band.

1). For this reason, hereafter all our discussion on the vibrational spectra will be based on the  $COO^-/NH_3^+$  form of Phe, Tyr, and Trp.

Stokes Raman spectra were collected by exciting 50  $\mu L$  of solution, placed in Suprasil quartz cells (5 mm path length), with the 488 nm line emitted by an  $Ar^+$  laser (Spectra Physics). The exciting power at the sample was ca. 200 mW. Scattered light at right angle was analyzed on a Jobin-Yvon T64000 spectrograph in a single spectrograph configuration with a 1200 grooves/mm holographic grating and a holographic notch filter. A liquid nitrogen cooled CCD detection system (Spectrum One, Jobin-Yvon) was used to collect Raman data. The effective spectral slit width was set to ca. 5  $cm^{-1}$ . FT-IR spectra were recorded on a Nicolet Magna 860 FT-IR spectrometer (ThermoFisher) equipped with a highly sensitive MCT detector, using a through plate crystal (ZnSe; incident angle 45°; 12.12  $\mu M$  effective path length). Spectra were collected with 1000 scans for Tyr and 500 scans for Phe and Trp, at a 4  $cm^{-1}$  resolution. Baseline correction and wavenumber determination of FT-IR spectra were performed using internal Omnic software. Post-processing of Raman spectra, including subtraction of buffer contribution, baseline correction, and smoothing, was performed by means of GRAMS/32 software (Galactic Industries). In order to facilitate the comparison between the different vibrational spectra, each of them has been normalized to the intensity of its most intense band. Final presentation of vibrational spectra has been performed by means of SigmaPlot package.

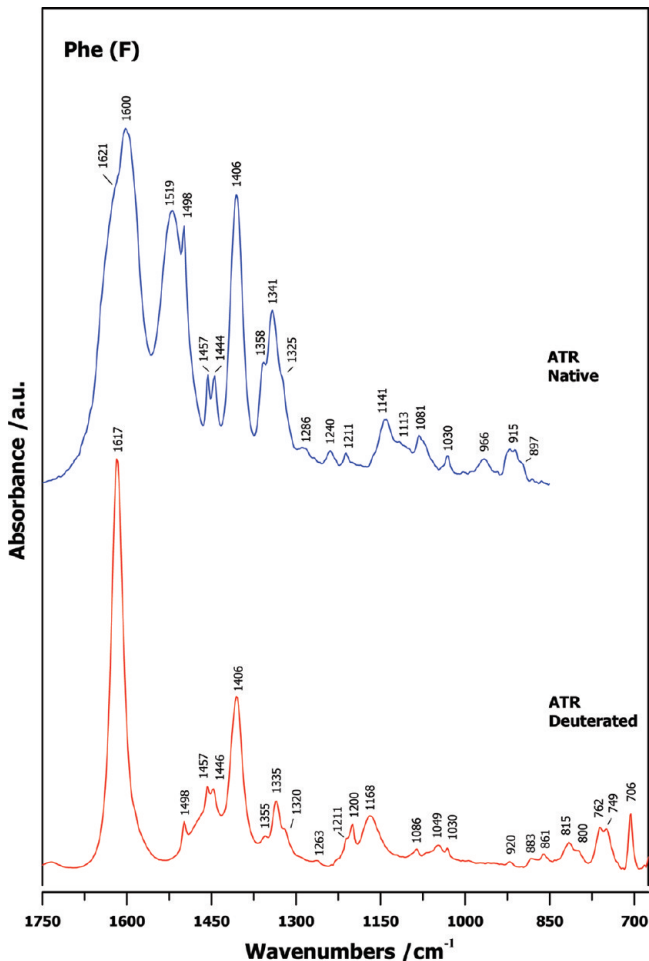


**Figure 3.** Room temperature FT-IR ATR spectra of phenylalanine observed in aqueous solutions: top,  $H_2O$  solution; bottom,  $D_2O$  solution. The intensity of each observed spectrum was normalized to its most intense peak.

**II.2. Theoretical Section.** Structural and vibrational data of the zwitterionic forms of the three AAs (Figure 1) were estimated by means of DFT calculations.<sup>42</sup> Theoretical calculations were performed by means of hybrid B3LYP functional, i.e., a combination of the Becke's three-parameter (B3) exchange functional<sup>43</sup> and Lee–Yang–Parr (LYP) nonlocal correlation functional.<sup>44</sup> To build up molecular orbital wave functions, linear combinations of atomic basis sets 6-31++G\*, represented by standard split valence double- $\zeta$  Gaussian functions enriched by d orbital functions on heavy atoms (C, N, and O) and diffuse functions on heavy and hydrogen atoms, were used. Numerical calculations were carried out with Gaussian03 pakage.<sup>45</sup> Each AA was hydrated by means of two distinct models: (i) an implicit model, by means of a polarizable dielectric continuum (COSMO),<sup>46,47</sup> capable of mimicking a bulk water environment around a molecule; and (ii) an explicit model, by a cluster of  $n$  water molecules surrounding a given AA and capable of building an acceptable H-bond network between water and all the acceptor ( $COO^-$ ) and donor ( $NH_3^+$ , NH, and OH) sites. Through our calculations in a continuum solvent, we have attempted to represent the energy landscapes of the three AAs by means of their potential energy surfaces (PESs), showing the variation of the electronic energy ( $E_e$ ) as a function of  $\chi_1$  and  $\chi_2$  torsion angles defined around  $C_\alpha-C_\beta$  and  $C_\beta-C_\gamma$  bonds of their side chains, respectively, as follows:  $\chi_1 = \varphi(N_t-C_\alpha-C_\beta-C_\gamma)$  and  $\chi_2 = \varphi(C_\alpha-C_\beta-C_\gamma-C_\delta)$  (Figure 1).  $E_e(\chi_1, \chi_2)$  values were

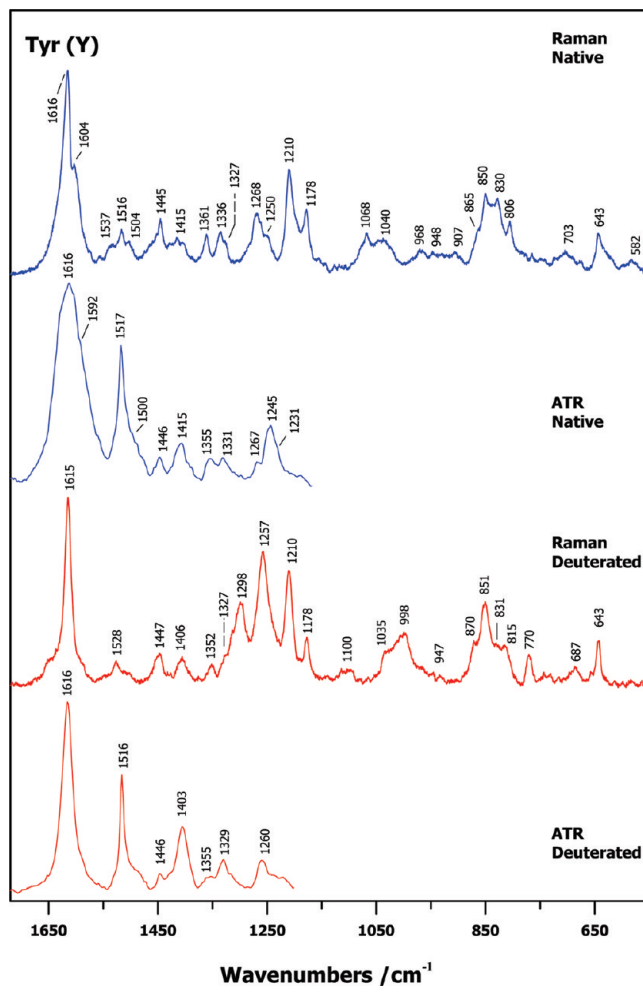


**Figure 4.** Room temperature vibrational spectra of tyrosine observed in aqueous solutions. From top to bottom: Raman spectrum ( $\lambda_L = 488$  nm) recorded in  $H_2O$  solution, FT-IR ATR spectrum in  $H_2O$  solution, Raman spectrum ( $\lambda_L = 488$  nm) recorded in  $D_2O$  solution, and FT-IR ATR spectrum in  $D_2O$  solution. Because of the very low water solubility of tyrosine (0.45 mg/mL at saturation), solution Raman and FT-IR spectra of this AA were obtained at very low concentration (2.3 mM, just below the saturation limit) and with a long accumulation time. The intensity of each spectrum was normalized to its most intense band.

calculated by a single-point approach through successive steps of  $15^\circ$  on each torsion angle.

### III. Results and Discussion

**III.1. Observed Spectra in  $H_2O$  and  $D_2O$ .** Raman and FT-IR spectra of the three AAs recorded in  $H_2O$  and  $D_2O$  solutions are presented in Figures 2–5. Here, we focus only on the  $1700$ – $600\text{ cm}^{-1}$  region which brings the most useful information on the backbone and side-chain vibrational modes of the studied AAs. The wavenumbers as well as the relative intensities of the main Raman and FT-IR bands are reported in Tables 1–3 for Phe, Tyr, and Trp, respectively. By examination of the spectra displayed in Figures 2–5, we can confidently assign them to the aqueous phase spectra of aromatic AAs, by considering first the changes observed in the Raman and FT-IR spectra upon deuteration on labile hydrogens (involved in the backbone  $NH_3^+$  group as well as in the side-chain OH and NH groups), proving a perfect water solubilization of all the three AAs. As mentioned in section II.1, the main problem encountered in the course of our experiments was the low water solubility of tyrosine. We have recorded the vibrational spectra

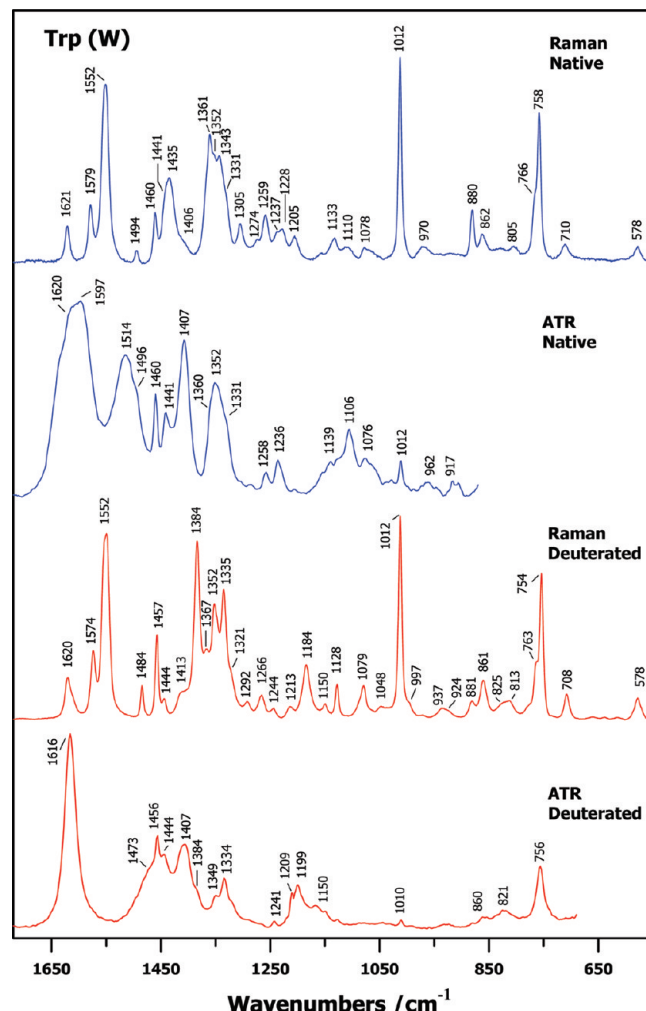


**Figure 5.** Room temperature vibrational spectra of tryptophan observed in aqueous solutions. From top to bottom: Raman spectrum ( $\lambda_L = 488$  nm) recorded in  $H_2O$  solution, FT-IR ATR spectrum in  $H_2O$  solution, Raman spectrum ( $\lambda_L = 488$  nm) recorded in  $D_2O$  solution, and FT-IR ATR spectrum in  $D_2O$  solution. The intensity of each spectrum was normalized to its most intense band.

of this AA in solid state (powder), as well as in the solutions with higher Tyr/water weight-to-weight ratios ( $R$ ) (a part of these data are reported in the Supporting Information, see Figure S1). Upon increasing  $R$ , the vibrational spectra resemble more and more those obtained from solid samples, because of the coexistence of nondissolved powder in water. Furthermore, in these conditions, the spectra recorded in  $H_2O$  and  $D_2O$  were quite similar, proving the inaccessibility of Tyr labile hydrogens, which presumably remain in solid phase with insufficient contact with solvent. On the basis of all the vibrational results that we could collect on Tyr in different conditions (pH, concentration, and temperature), we can now conclude that the previously reported FT-IR spectra recorded as it was claimed, at a theoretical molar concentration of 100 mM, and at different pH values (0, 11, 13),<sup>33</sup> arise mainly from nondissolved powder of Tyr, rather than from its aqueous solutions. In fact, variation of solution pH or temperature does not seem to increase considerably the water solubility of this AA. On the other hand, Raman spectra recorded in aqueous solutions present the same intense bands as those previously observed by SERS.<sup>34</sup> It is to be noted that the SERS method is generally reputed for using less concentrated samples compared to classical Raman scattering analyzed in aqueous solution. Unfortunately, no sufficient detail

TABLE 1: Vibrational Modes of Phenylalanine in Aqueous Solutions ( $H_2O$  and  $D_2O$ ) and Their Assignments<sup>a</sup>

| Raman<br>H <sub>2</sub> O        | IR<br>H <sub>2</sub> O | calcd<br>Phe + 5H <sub>2</sub> O  | assignments (PED %)              | Raman<br>D <sub>2</sub> O         | IR<br>D <sub>2</sub> O   | Phe + 5D <sub>2</sub> O   | calcd<br>assignments (PED %) |
|----------------------------------|------------------------|---|----------------------------------|-----------------------------------|--|---|------------------------------|
| 1621 (s)<br>1606 (s)<br>1586 (s) | 1745<br>1686<br>1654   | NH <sub>3</sub> <sup>+</sup> asym bend (34); NH <sub>3</sub> <sup>+</sup> asym bend (13)<br>CHOO <sup>-</sup> asym st (35); NH <sub>3</sub> <sup>+</sup> asym bend (29)<br>Cδ1-Cε1 (21); Cδ2-Cε2 (20) | 1617 (s)<br>1606 (s)<br>1586 (s) | 1617 (s)<br>1498 (m)<br>1458 (sh) | 1697<br>1654<br>1632   | CtOO <sup>-</sup> asym st (84)<br>Cδ1-Cε1 (21); Cδ2-Cε2 (20)<br>Cε2-Cζ (19); Cε1-Cζ (18); Cy-Cδ1 (14) |                              |
| 1519 (s)<br>1498 (s)             | 1632<br>1567           | NH <sub>3</sub> <sup>+</sup> sym bend (38); NH <sub>3</sub> <sup>+</sup> sym rock (36)<br>Cδ1-Cε1-H (12); Cδ2-Cε2-H (11); Cδ1-Cε1-H (10); Cε2-Cδ2-H (9)   | 1498 (m)                         | 1538                              | Cδ1-Cε1-H (12); Cδ2-Cε2-H (11); Cε1-Cδ1-H (10); Ce2-C02-H (9)                              |   |                              |
| 1458 (sh)<br>1457 (m)            | 1502                   | Cβ-bend (84)  | 1457 (m)                         | 1502                              | Cβ-bend (87)   |   |                              |
| 1446 (m)                         | 1492                   | Cε1-Cζ-H (11); Cε2-Cζ-H (11); Cε2-Cε1-H (10); Cβ-bend (10); Cε2-Cε2-H (9)   | 1446 (m)                         | 1492                              | Cε1-Cζ-H (12); Cε2-Cζ-H (11); Cε2-Cε1-H (10); Cε2-Cε2-H (10); Cβ-bend (8)                  |   |                              |
| 1413 (m)<br>1406 (sh)            | 1414<br>1399           | Nt-Cα-H (39); Cβ-Cα-H (23); NH <sub>3</sub> <sup>+</sup> asym rock (8); Cβ-rock (8)<br>Cβ-rock (26); CtOO <sup>-</sup> sym st (13); Nt-Cα-H (11); Ct-Cα-H (10)  | 1446 (m)<br>1406 (s)             | 1405                              | Cβ-Cα-H (27); Cβ-rock (25); Nt-Cα-H (15); Cβ-twist (8)                                     |   |                              |
| 1360 (m)                         | 1373                   | CtOO <sup>-</sup> sym st (38)   | 1408 (m)<br>1356 (m)             | 1385                              | CtOO <sup>-</sup> sym st (55); Ct-Cα (11); Nt-Cα-H (15)                                    |   |                              |
| 1339 (m)                         | 1366                   | Cγ-Cδ1-H (12); CtOO <sup>-</sup> sym st (11); Cγ-Cδ2-H (11); Cε1-Cδ1-H (9)  | 1355 (sh)<br>1335 (m)            | 1368                              | Cγ-C01-H (14); Cγ-C02-H (14); Cε1-Cδ1-H (10); Ce2-C02-H (10)                               |   |                              |
| 1327 (sh)                        | 1352                   | Cγ-Cδ1 (13); Cy-C02 (13); Cβ-twist (10); Cε2-Cζ (9); Cδ1-Cε1 (9); Cδ2-Cε2 (8); Cε1-Cζ (8)   | 1320 (sh)                        | 1361                              | Cβ-C01 (13); Cy-C02 (12); Cβ-twist (9); Cε1-Cζ (8); Ce2-Cζ (8); Cδ2-Cε2 (8)                |   |                              |
| 1286 (w)                         | 1304                   | Cβ-rock (27); Cβ-Cα-H (19); Cβ-twist (14); Ct-Cα-H (12)   | 1298 (sh)                        | 1351                              | Ct-Cα-H (33); Cβ-rock (19); Cβ-Cα-H (13); Nt-Cα-H (10)                                     |   |                              |
| 1240 (w)                         | 1272                   | NH <sub>3</sub> <sup>+</sup> asym rock (21); Cβ-twist (21); Ct-Cα-H (14)  | 1262 (m)<br>1207 (s)             | 1290<br>1227                      | NtD <sub>3</sub> <sup>+</sup> asym bend (35); Cβ-twist (20)                                |   |                              |
| 1227                             | 1227                   | Cβ-Cγ (36); Cβ-rock (8)   | 1263 (w)<br>1211 (sh)            | 1238                              | Cβ-Cγ (36)   |   |                              |
| 1207 (s)                         | 1211 (w)               | Cδ1-Cε1 (10); Cδ1-Cε1-H (10); Cε2-Cε1-H (10); Cδ2-Cε2 (9); Cε2-Cε2-H (8)  | 1200 (m)                         | 1214                              | NtD <sub>3</sub> <sup>+</sup> asym bend (27); NdD <sub>3</sub> <sup>+</sup> asym bend (13) |   |                              |
| 1184 (m)                         | 1192                   | NH <sub>3</sub> <sup>+</sup> asym rock (32); Ct-Cε1-H (25)  | 1183 (m)                         | 1212                              | Cδ2-Cε2 (9); C01-Cε1-H (9); Cε2-Cε2-H (8)  |   |                              |
| 11160 (m)                        | 1191                   | Cε2-Cζ-H (17); Cε1-Cζ-H (16); Cδ2-Cε2-H (10); Cδ1-Cε1-H (9); Cε2-Cε2-H (9)  | 1168 (m)                         | 1191                              | Cε2-Cζ-H (18); Cε1-Cζ-H (17); Cε2-Cε2-H (10); Cδ2-Cε2-H (10);                              |   |                              |
| 1141 (m)                         | 1148                   | Cβ-twist (23); NH <sub>3</sub> <sup>+</sup> asym rock (10)  | 1090 (w)                         | 1127                              | Cε2-Cε2-H (8)  |   |                              |
| 1113 (sh)                        | 1098                   | Cδ2-Cε2 (9); Cε1-Cδ1-H (8); Cε2-Cδ2-H (8)   | 1063 (w)                         | 1093                              | Cδ1-Cε1-H (9); Cε2-Cε1-H (8); Cε2-Cε2-H (8)  |   |                              |
| 1081 (m)                         | 1072                   | Cα-Cβ (28); Nt-Cα (22); NH <sub>3</sub> <sup>+</sup> asym rock (11)   | 1049 (w)                         | 1054                              | Cα-Cβ (18); Cε2-Cδ2-H (8)  |   |                              |
| 1030 (w)                         | 1054                   | Cε1-Cζ (20); Cε2-Cζ (18); Cε2-Cε1-H (8); Cε2-Cε2-H (8)  | 1030 (w)                         | 1025                              | Cε2-Cε2-H (20); Cε2-Cε1-H (8); Cε2-Cε2-H (8)   |   |                              |
| 1004 (s)                         | 1016                   | Cγ-Cδ1 (8); Cγ-Cδ2 (8); Cγ-Cδ2-Cε2 (8); Cε1-Cε1-Cδ1 (8)   | 1004 (s)                         | 1015                              | Cα-Cβ (25); Cε2-Cε2-H (8)  |   |                              |
| 993 (sh)                         | 1004                   | ω(Cε1-Cε1) (22); ω(Cε2-H) (18); ω(Cε1-H) (16); τ(Cε2-Cε1) (11); τ(Cε1-Cε1) (10)   | 993 (sh)                         | 1003                              | ω(Cε2-H) (22); ω(Cε2-H) (18); ω(Cε1-H) (16); τ(Cε2-Cε1) (11); τ(Cε1-Cε1) (10)              |   |                              |
| 971 (w)                          | 985                    | ω(Cδ1-H) (19); ω(Cε1-H) (18); ω(Cε2-H) (18); ω(Cδ2-H) (15)  | 985                              | 985                               | ω(Cδ1-H) (19); ω(Cε1-H) (18); ω(Cε2-H) (18); ω(Cδ2-H) (15)                                 |   |                              |
| 966 (w)                          | 953                    | Cβ-wag (17); W...W  | 921 (w)                          | 929                               | ω(Cδ2-H) (24); ω(Cε1-H) (22); ω(Cδ1-H) (21)  |   |                              |
| 951 (m)                          | 934                    | ω(Cδ2-H) (21); ω(Cδ1-H) (19); ω(Cε1-H) (17)   | 882 (w)                          | 869                               | Cβ-wag (21); Cα-Ct (10)  |   |                              |
| 922 (w)                          | 917                    | Cα-Ct (19); W...W   | 883 (w)                          | 865                               | ω(Cδ2-H) (17); ω(Cε1-H) (16); ω(Cδ1-H) (16); ω(Cε2-H) (14)                                 |   |                              |
| 897 (sh)                         | 866                    | ω(C01-H) (18); ω(Cε1-H) (17); ω(Cδ2-H) (16)   | 857 (sh)                         | 833                               | Cβ-Cγ (15); Cε1-Cζ-Cε2 (8)   |   |                              |
| 826 (sh)                         | 854                    | Nt-Cα (25); Cβ-wag (23)   | 838 (w)                          | 823                               | Nt-Cα (16); OCIO (11)  |   |                              |
| 817 (w)                          | 834                    | Cε1-Cε1 (16); Cε1-Cε1 (8); Cε1-Cε1-Cε2 (8)  | 814 (m)<br>798 (m)               | 822                               | NtD <sub>3</sub> <sup>+</sup> asym rock (23); NtD...OCl                                    |   |                              |
| 774                              | 771 (m)                | CαC1O <sup>-</sup> sym bend (9); OCIO (9); Nt-Cα-Ct (9); Nt-Cα (8)  | 815 (m)<br>759 (sh)              | 765                               | ω(Cε1-H) (21); ω(Cδ2-H) (8); ω(Cβ-Cγ) (8); NtH...OCl                                       |   |                              |
| 751 (m)                          | 764                    | ω(Cε1-H) (23); Cδ2-Cε1-H (17); Cδ1-Cε1-Cε2 (16); Cy-Cδ1-Cε1 (12); Cy-Cδ2-Cε2 (11)   | 800 (sh)<br>741 (m)              | 748                               | Nt-Cα (11); (NtH...OCl)  |   |                              |
| 713                              | 713                    | ω(Cε1-H) (20); ω(Cβ-Cγ) (10); τ(Cγ-Cδ1) (8); τ(Cγ-Cδ1) (8)  | 706 (m)                          | 713                               | ω(Cε1-H) (20); ω(Cε2-H) (20); ω(Cβ-Cγ) (10); τ(Cγ-Cδ1) (8)                                 |   |                              |
| 654                              | 634                    | OCIO (16); Cβ-scissor (9); τ(Nt-Cα) (8); Ct-Cα (8); NtH...OCl   | 622 (m)                          | 651                               | OCIO (12); Ca-Ct (9); Cβ-scissor (9); NtD...OCl  |   |                              |
| 632 (sh)                         | 571                    | Cε1-Cε2-Cδ2 (17); Cδ1-Cε1-Cε2 (17); Cy-Cδ1-Cε1 (12); Cy-Cδ2-Cε2 (11)  |                                  | 634                               | Cε1-Cε2-Cδ2 (17); Cδ1-Cε1-Cε2 (17); Cy-Cδ1-Cε1 (12); Cy-Cδ2-Cε2 (11)                       |   |                              |
| 632 (m)                          | 536                    | Cδ2-Cε2-Cδ1 (15); Cε1-Cε2-Cε2 (8); Ca-Ct (8)  |                                  | 565                               | Cδ2-Cε2-Cδ1 (13); Ca-Ct (9)  |   |                              |
| 552 (w)                          |                        | CαC1O <sup>-</sup> asym bend (15); ω(Cβ-Cγ) (13); W...W   |                                  | 532                               | CaC1O <sup>-</sup> asym bend (19); ω(Cβ-Cγ) (18)   |   |                              |

<sup>a</sup> s, strong; m, medium; w, weak; sh, shoulder. Calcd.: Calculated wavenumbers from the lowest energy conformer (Figure 7 bottom) of phenylalanine surrounded by five water molecules. See Table 4 for energy values. The angular bending modes of the tetrahedron located on the  $C_p$  atom of the side chain are referred to as bending (-bend), wagging (-wag), twisting (-twist), rocking (-rock), and scissoring (-scissor).  $\omega$  and  $\tau$  designate an out-of-plane bending or a torsional internal coordinate, respectively. W = water. For atom numbering, see Figure 1.

**TABLE 2: Vibrational Modes of Tyrosine in Aqueous Solutions ( $H_2O$  and  $D_2O$ ) and Their Assignments<sup>a</sup>**

| Raman<br>$H_2O$ | IR<br>$H_2O$  | calcd<br>Tyr + 7 $H_2O$   | assignments (PED %) | Raman<br>$D_2O$ | IR<br>$D_2O$   | calcd<br>Tyr + 7 $D_2O$ | assignments (PED %)   |
|-----------------|---|---|---------------------|-----------------|--|-------------------------|---|
| 1749            | COO <sup>-</sup> asym st (35); NH <sub>3</sub> <sup>+</sup> asym bend (11)                    |   |                     |                 |  |                         |   |
| 1725            | NH <sub>3</sub> <sup>+</sup> asym bend (43)   |   |                     |                 |  |                         |   |
| 1604 (sh)       | 1592 (sh)   | COO <sup>-</sup> asym st (28); NH <sub>3</sub> <sup>+</sup> asym bend (20)                              |                     | 1616 (s)        | 1616 (s)   | 1737                    | CtOO <sup>-</sup> asym st (8); CtOO <sup>-</sup> sym st (11)  |
| 1616 (s)        | 1616 (s)  | Cel-Cε1 (19); Cε2 (18); Cε1-Cε2 (10); Cε2-Cε2 (10)  |                     | 1664            | Cδ1-Cε1 (20); Cδ2-Cε2 (19); Cy-Cε1 (8); Ce2-Cε2 (8)  |                         |   |
| 1537 (sh)       | 1665  | Cε1-Cε2 (22); Cy-Cε2 (18); Cε2-Cε2 (15); Cy-Cε1 (13)  |                     | 1630            | Cε1-Cε2 (22); Cy-Cε2 (17); Ce2-Cε2 (17); Cy-Cε1 (13) |                         |   |
| 1504 (sh)       | 1500 (sh)   | NH <sub>3</sub> <sup>+</sup> sym bend (33); NH <sub>3</sub> <sup>+</sup> sym rock (26)                  |                     |                 |  |                         |   |
| 1516 (m)        | 1517 (s)  | Cδ1-Cε1-H (10); Ce2-Cε2-H (8)   |                     |                 |  |                         |   |
| 1445 (m)        | 1446 (w)  | Cβ-bend (93)  |                     |                 |  |                         |   |
| 1415 (w)        | 1415 (m)  | Cε2-Cε2-H (11); Cδ2-Cε2 (10); Cε2-Cε1-H (8); Cγ-Cε1-H (8)   |                     | 1447 (m)        | 1446 (w)   | 1502                    | Cδ1-Cε1-H (9); Ce1-Cε1-H (9); Ce2-Cε2-H (9); Cd2-Cε2 (94)   |
|                 |   |   |                     | 1406 (w)        | 1403 (s)   | 1468                    | Cδ2-Cε2 (12); Cy-Cε1-H (11); Cy-Cε2-H (11); Cd1-Cε1 (10); Cε2-Cε1 (10)  |
|                 |   |   |                     |                 |  | 1391                    | Cβ-rock (52); Cβ-Cα-H (16)  |
| 1392            | Cβ-rock (44); Cβ-Cα-H (17)  |   |                     |                 |  |                         |   |
| 1390            | Cε1-O-H (14); Cd1-Cε1 (9); Cy-Cε2-H (8)   |   |                     |                 |  |                         |   |
| 1386            | Nt-Cα-H (40); Cβ-twist (8)  |   |                     |                 |  |                         |   |
| 1355 (w)        | 1355 (w)  | Nt-Cα-H (40); Cβ-twist (8)  |                     | 1352 (w)        | 1355 (w)   | 1377                    | Nt-Cα-H (30); Cβ-twist (17)   |
| 1336 (m)        | 1331 (w)  | Cy-Cε2 (10); Cy-Cε1 (9); Nt-Cα-H (8); Cβ-twist (8)  |                     | 1327 (sh)       |  | 1350                    | Cε1-Cε2 (15); Ce2-Cε2 (12); Ce2-Cε2-H (9)   |
|                 |   | CIO <sup>-</sup> sym st (39); Cβ-rock (15)  |                     | 1298 (s)        | 1329 (m)   | 1333                    | CtOO <sup>-</sup> sym st (38); Ni-Cα-H (19); Cβ-rock (10)   |
| 1327 (sh)       | 1331 (w)  | Cε1-Cα-H (20); CIO <sup>-</sup> sym st (16); NH <sub>3</sub> <sup>+</sup> asym rock (15); Cβ-Cα-H (10); |                     |                 |  |                         |   |
| 1268 (s)        | 1267 (w)  | Cε2-O (42); Cε2-Cε2 (10); Cε1-Cε2 (9)   |                     | 1257 (s)        | 1260 (m)   | 1285                    | Cε2-O (25)  |
| 1250 (sh)       | 1245 (m)  | Cε2-O-H (25); Ce2-Cε2 (11)  |                     |                 |  | 1241                    | NtD <sub>3</sub> <sup>+</sup> asym bend (49)  |
| 1231 (sh)       | 1231 (sh)   | Cβ-Cγ (23); Cβ-rock (13); Cβ-twist (11); Cy-Cε1-H (9)   |                     |                 |  | 1240                    | NtD <sub>3</sub> <sup>+</sup> asym bend (14); NtD <sub>3</sub> <sup>+</sup> sym bend (10); NtD <sub>3</sub> <sup>+</sup> sym rock (8) |
| 1210 (s)        | 1219  | Cβ-twist (28); Cβ-Cγ (12); Cy-Cε2-H (8)   |                     | 1210 (s)        |  | 1213                    | Cβ-twist (21); W (DOD) (8)  |
| 1178 (m)        | 1208  | Cδ1-Cε1-H (13); Cε2-Cε2-H (10); Cδ2-Cε2-H (9); Cy-Cε1-H (9);  |                     | 1178 (m)        |  | 1207                    | Cδ1-Cε1-H (11); Cy-Cε2-H (9); Cδ2-Cε2-H (9); Cε2-Cε2-H (8)  |
|                 |   | Cε1-Cε1-H (8); Cy-Cε2-H (8); Cε1-Cε1-H (8)  |                     |                 |  |                         |   |
| 1148            | NH <sub>3</sub> <sup>+</sup> asym rock (15); Cβ-Cα-H (8); Cδ2-Cε2-H (8)                       |   |                     | 1100 (w)        |  | 1143                    | Cδ2-Cε2-H (19); Cd1-Cε1-H (12); Cε2-Cε2-H (11); Cδ2-Cε2 (11); Cε1-Cδ1-H (9)   |
|                 |   |   |                     |                 |  |                         |   |
| 1135            | NH <sub>3</sub> <sup>+</sup> asym rock (11); Cd2-Cε2-H (10); Cε2-Cε2-H (8); Cd1-Cε1-H (8)     |   |                     |                 |  |                         |   |
| 1096 (m)        | 1096  | NH <sub>3</sub> <sup>+</sup> asym rock (38); Cε1-Cα-H (13)  |                     |                 |  |                         |   |
| 1040 (m)        | 1034  | Cγ-Cδ2-Cε2 (12); Cε2-Cε2-H (12); Cd1-Cε1-Cε1 (11); Cε1-Cε1-H (10);                                      |                     | 1035 (sh)       |  | 1066                    | Cα-Cβ (35); Ni-Cα (9)   |
|                 |   | Cγ-Cε2-Cε2 (10); Cε2-Cε2-Cε2 (10); Cy-Cε2-H (8)   |                     |                 |  | 1034                    | Cγ-Cδ1-Cε1 (11); Cy-Cε2-Cε2-Cε2 (11); Cd1-Cε1-Cε1 (11); Cε1-Cε1-H (10);   |
| 1028            | Nt-Cα (21); Cβ-wag (13); NH <sub>3</sub> <sup>+</sup> asym rock (11); Cβ-Cα-Ct (8); Ca-Cβ (8) |   |                     | 998 (s)         |  | 1023                    | Cε2-Cε2-Cε2 (10); Cε2-Cε2-Cε2 (10); Cε1-Cε1 (8); Ni-Cα (11); Ni-Cα-Cβ (8)   |
|                 |   |   |                     |                 |  | 987                     | Cε1-Cε1-D (52)  |
| 968 (w)         | 986   | Ca-Cβ (13); W(H)...O(Ct)  |                     | 947 (w)         |  | 980                     | ω(Cδ2-H) (33); ω(Cε2-H) (15); τ(Cδ2-Cε2) (12)   |
| 948 (w)         | 979   | ω(Cδ2-H) (37); ω(Cε2-H) (20); τ(Cδ2-Cε2) (16)   |                     |                 |  | 976                     | ω(Cδ1-H) (22); NtD <sub>3</sub> <sup>+</sup> asym rock (9); ω(Cε1-H) (8)  |
|                 | 962   | ω(Cδ1-H) (37); ω(Cε1-H) (16); τ(Cδ1-Cε1) (14)   |                     |                 |  | 953                     | ω(Cδ1-H) (25); τ(Cδ1-Cε1) (13); ω(Cε1-H) (11)   |
| 907 (w)         | 955   | Ca-Cβ (11); Cβ-wag (9)  |                     |                 |  | 874                     | Cβ-wag (28); Ca-Ct (18); Ni-Cα (15); OCIO (9)   |
| 865 (sh)        | 890   | Nt-Cα (13); Cβ-wag (9); (W)H...O(Ct)  |                     |                 |  | 855                     | ω(Cε2-H) (17); ω(Cε2-O) (8); ω(Cδ2-H) (8)   |
| 850 (s)         | 864   | ω(Cε2-H) (9); ω(Cε2-H) (11); ω(Cδ2-H) (11); ω(Cε2-H) (14); ω(Cε2-Cε2) (9)                               |                     |                 |  | 849                     | ω(Cε2-H) (14); ω(Cδ2-H) (18); ω(Cε2-Cε2) (8)  |
| 830 (s)         | 850   | ω(Cε2-H) (9); ω(Cδ1-H) (16); ω(Cε2-H) (8)   |                     |                 |  | 831                     | ω(Cε1-H) (37); ω(Cδ1-H) (18); ω(Cε2-H) (9); τ(Cε1-Cε2) (8)  |
| 806 (s)         | 831   | ω(Cε1-H) (33); ω(Cδ1-H) (16); ω(Cε2-H) (8)  |                     |                 |  | 820                     | NtD <sub>3</sub> <sup>+</sup> asym rock (30); Ca-Cβ (17); W(O)...D(Nt)  |
|                 |   |   |                     |                 |  |                         |   |
| 790             | OCHO (16); Nt-Cα (10); Ca-Cβ (8)  |   |                     | 770 (m)         |  | 788                     | OCTO (25); Ni-Cα (18); Ca-CtO (18); Cε1-Cε2-Cε2 (9); Cε2-Cε2-Cε2 (9); τ(Ni-Cα) (8)  |
|                 |   |   |                     |                 |  | 733                     | Cβ-Cγ (18); Cε1-Cε2-Cε2 (9); Cε2-Cε2-Cε2 (9); τ(Ni-Cα) (8)  |
| 736             | Cβ-Cγ (19); Cε1-Cε2-Cε2 (10); Cε2-Cε2 (8); τ(Ni-Cα) (8)                                       |   |                     |                 |  | 723                     | ω(Cε2-O) (15); ω(Cβ-Cγ) (12); τ(Cδ1-Cε1) (9); τ(Cδ2-Cε2) (9)  |
| 727             | ω(Cβ-Cγ) (17); ω(Cε1-Cε2) (16); τ(Cδ1-Cε1) (9); τ(Cδ2-Cε2) (9)                                |   |                     |                 |  | 653                     | Cγ-Cδ1-Cε1 (13); Cγ-Cε2-Cε2 (12); Cδ1-Cε1-Cε1 (10); Cε1-Cε1-Cδ1 (10)  |
| 703 (w)         | 643 (s)   | Cγ-Cδ1-Cε1 (13); Cγ-Cε2-Cε2 (12); Cδ1-Cε1-Cε1 (10); Cε1-Cε1-Cδ1 (10)                                    |                     | 687 (w)         |  |                         |   |
| 582 (w)         | 595   | Ca-Ct (14); OCTO (10); Ni-Cα-Ct (8)   |                     | 643 (s)         |  |                         |   |

<sup>a</sup> S, strong; m, medium; w, weak; sh, shoulder. Calcd.: Calculated wavenumbers from the lowest energy conformer (Figure 8 bottom) of tyrosine surrounded by seven water molecules. See Table 4 for energy values. The angular bending modes of the tetrahedron located on the C<sub>β</sub> atom of the side chain are referred to as bending (-bend), wagging (-wag), twisting (-twist), rocking (-rock), and scissoring (-scissor). ω and τ designate an out-of-plane bending and a torsional internal coordinate, respectively. W = water. For atom numbering, see Figure 1.

TABLE 3: Vibrational Modes of Tryptophan in Aqueous Solutions ( $\text{H}_2\text{O}$  and  $\text{D}_2\text{O}$ ) and Their Assignments<sup>a</sup>

| Raman<br>H <sub>2</sub> O | IR<br>H <sub>2</sub> O | calcd<br>Trp + 6H <sub>2</sub> O | assignments (PED %)  | Raman<br>D <sub>2</sub> O       | IR<br>D <sub>2</sub> O | calcd<br>Trp + 6D <sub>2</sub> O | assignments (PED %)   |
|---------------------------|------------------------|----------------------------------|--|---------------------------------|------------------------|----------------------------------|---|
| 1621 (m)                  | 1620 (s)               | 1746<br>1695                     | NH <sub>3</sub> <sup>+</sup> asym bend (45); W(HOH) (13)<br>NH <sub>3</sub> <sup>+</sup> asym bend (38); W(HOH) (17)<br>Cε2-Cε2' (20); Cε3-Cε3' (14); Cδ2-Cε3' (8)   | 1620 (m)                        | 1616 (s)               | 1674<br>1660                     | CtOO <sup>-</sup> asym st (87)<br>Cε2-Cε2' (20); Cε3-Cε3' (15); Cδ2-Cε3' (10); Cε2-Cη (8)   |
| 1597 (m)                  | 1597 (s)               | 1660<br>1617                     | COO <sup>-</sup> asym st (53); W(HOH) (24)<br>Cδ2-Cε3' (15); Cε2-Cη (14); Cε3-Cη (13)  | 1574 (s)                        | 1611                   | 1611                             | Cε3-Cη (16); Cδ2-Cε3' (14); Cε2-Cη (12); Cδ2-Cε2' (9)   |
| 1552 (s)                  | 1514 (s)               | 1607<br>1589                     | NH <sub>3</sub> <sup>+</sup> sym bend (32); NH <sub>3</sub> <sup>+</sup> sym rock (33)<br>Cγ-Cδ1 (33); Cε2-Cε2' (10); Cβ'-Cγ (8)                                     | 1552 (s)                        | 1589                   | 1589                             | Cγ-Cδ1 (35); Cε2-Cε2' (9); Cβ'-Cγ (9)   |
| 1496 (w)                  | 1494 (w)               | 1529<br>1499                     | Cη-Cε3-H (16); Cε3-Cε3' (9); Cε3-Cη-H (8)<br>Cβ'-bend (91)   | 1484 (m)<br>1457 (s)            | 1518<br>1500           | 1518<br>1489                     | Cη-Cε3-H (18); Cε3-Cε3' (13); Cε3-Cε3' (9)<br>Cβ'-bend (93)<br>Cδ2-Cε3-H (12); Cε2-Cε2' (8); Cδ2-Cε2' (8); Cε3-Cε3-H (8); Cε3-Cε3-H (8) |
| 1460 (m)                  | 1460 (s)               | 1493                             | Cδ2-Cε3-H (12); Cε2-Cε2' (10); Cε3-Cε3' (9); Cη-Cε2-H (8)  | 1444 (w)                        | 1444 (s)               | 1444 (s)                         | (8)   |
| 1435 (s)                  | 1435 (s)               | 1472<br>1426                     | Cε2-Nε1-H (15); H-Nε1-Cδ1 (13); Cδ2-Cγ (8)<br>CtOO <sup>-</sup> sym st (32); Cβ'-rock (10); Ca-Ct (10)   | 1413 (sh)<br>1384 (s)           | 1407 (s)<br>1384 (sh)  | 1430<br>1414                     | CtOO <sup>-</sup> asym st (15); Cβ'-twist (10); Cβ'-rock (9); Cδ2-Cγ (9)  |
| 1361 (s)                  | 1360 (sh)              | 1404<br>1388                     | Nt-Ca-H (30); Cβ-Cα-H (21); Cβ'-rock (17)<br>CtOO <sup>-</sup> sym st (14); Cδ2-Cγ (11); Cβ'-twist (8)   | 1367 (m)<br>1352 (s)            | 1349 (sh)<br>1334 (m)  | 1396<br>1383                     | CtOO <sup>-</sup> sym st (21); Cβ'-rock (8); Nt-Ca-H (12); Cδ2-Cε2' (8); Cδ2-Cε3' (8)   |
| 1343 (s)                  | 1331 (sh)              | 1382<br>1367                     | Cδ2-Cε2' (14); Cε2-Cη (12); Cε2-Cε3 (11); Cε3-Cε3' (8)<br>Cβ'-rock (25); Nt-Ca-H (15); CtOO <sup>-</sup> sym st (15)   | 1335 (s)                        | 1334 (m)               | 1366                             | Cε2-Nε1 (12); Cδ2-Cε2' (10); Cε2-Cη (9)   |
| 1338                      | 1338                   | 1338<br>1329                     | Ct-Ca-H (17); NH <sub>3</sub> <sup>+</sup> asym rock (14); CtOO <sup>-</sup> sym st (11); Cβ'-Ca-H (10)<br>Cβ'-rock (15); Cε2-Nε1 (12); Cδ2-Cγ (8); Cε2-Nε1 (8)      | 1321 (sh)<br>1292 (w)           | 1348<br>1324           | 1348<br>1324                     | Nt-Ca-H (40); Cβ'-rock (19); CtOO <sup>-</sup> sym st (8)   |
| 1305 (w)                  | 1295 (m)               | 1239<br>1239                     | Cε2-Nε1 (16); Cε2-Cε3-H (12); Cε2-Cε3-H (10); Cβ'-twist (10)   | 1266 (w)<br>1244 (w)            | 1241 (w)<br>1233 (w)   | 1274<br>1233                     | Ct-Ca-H (16); Cβ'-twist (11); Cβ'-Ca-H (10)   |
| 1274 (sh)                 | 1259 (m)               | 1237 (w)<br>1236 (m)             | Cε2-Nε1 (16); Cε2-Cε3-H (12); Cε2-Cε3-H (10); Cβ'-twist (10)   | 1213 (w)<br>1209 (sh)           | 1227<br>1227           | 1227                             | NtD <sub>3</sub> <sup>+</sup> sym bend (47); Nd <sub>3</sub> <sup>+</sup> sym rock (17); Cβ'-twist (15)                                 |
| 1228 (w)                  | 1228 (w)               | 1186<br>1181                     | Cε3-Cε3-H (16); Cη-Cε3-H (14); Cε3-Cη-H (10); Cε2-Cη-H (8)<br>Ct-Ca-H (23); NH <sub>3</sub> <sup>+</sup> asym rock (12); NH <sub>3</sub> <sup>+</sup> asym rock (11) | 1184 (m)<br>1150 (w)            | 1199 (m)<br>1150 (w)   | 1208<br>1201                     | NtD <sub>3</sub> <sup>+</sup> asym bend (47); Nd <sub>3</sub> <sup>+</sup> sym bend (8)   |
| 1205 (w)                  |                        | 1161<br>1161                     | NH <sub>3</sub> <sup>+</sup> asym rock (10); Cη-Cε2-H (8)<br>NH <sub>3</sub> <sup>+</sup> asym rock (13); Cε2-Nε1 (14); Cγ-Cδ1-H (8)                                 | 1079 (m)<br>1048 (w)            | 1176<br>1152           | 1176<br>1152                     | Nt-Cd <sub>1</sub> -H (15); Cε2-Cη-H (9); Nε1-Cδ1-H (9)<br>Cε3-Cε3-H (14); Cη-Cε3-H (9); Cε2-Cη-H (11); Cε2-Cη (8)                      |
| 1133 (w)                  | 1139 (sh)              | 1128<br>1110 (w)                 | Nε1-Cδ1-H (22); Cε2-Nε1 (14); Cγ-Cδ1-H (8)   | 1010 (w)                        | 1010 (w)               | 1110                             | Cα-Cβ (18)  |
| 1078 (w)                  | 1076 (m)               | 1048<br>1074                     | Nt-Ca (29); Co-Cβ (22); Cβ'-awag (8)<br>Cε3-Cη (34); Cε2-Cη (11); Cε3-Cε3' (9)   | 1012 (s)                        | 1012 (s)               | 1073<br>1022                     | Cα-Cβ (13); Nt-Ca (9); Nt-Ca-Ct (9)   |
| 1012 (s)                  | 1012 (w)               | 1038                             | Cβ'-Cγ (14); Nε1-Cδ1-Cγ (8)  | 997 (sh)                        | 997 (sh)               | 1073<br>990                      | Cε3-Cη (33); Cε3-Cε3' (11); Cε3-Cε3' (9)  |
| 970 (w)                   |                        | 974                              | ω(Cε3-H) (26); ω(Cη-H) (21); τ(Cε3-Cε3) (14); τ(Cε2-Cη) (13)   | 937 (w)<br>924 (sh)             | 948<br>936             | 1073<br>924                      | Cδ1-Nε1-D (23); Cε2-Nε1-D (9); W(O)••D(Nε1) (11)<br>ω(Cε3-H) (24); ω(Cε2-H) (20); ω(Cη-H) (16); τ(Cε2-Cη) (13); τ(Cε2-Cη) (8)           |
| 962 (w)                   | 949<br>936             | 907<br>891                       | Cβ'-wag (21); Cα-Cβ (13); NH <sub>3</sub> <sup>+</sup> asym rock (10); Ca-Ct (9)<br>ω(Cε3-H) (25); ω(Cε2-H) (20); ω(Cη-H) (16); τ(Cε2-Cε3) (11)                      | 881 (w)<br>861 (m)              | 868<br>863             | 876<br>863                       | Cβ'-wag (24); Nt-Ca (12); Ca-Ct (11); ω(Cδ1-H) (8)  |
| 917 (w)                   |                        | 880 (m)<br>862 (w)               | Nt-Cα (22); Cβ'-wag (11); Ca-Ct (9); (w)H••Nt (10)<br>Cε3-Cε3-Cη (12); Cε2-Nε1-Cδ1 (12)  | 861 (m)                         | 860 (w)                | 876<br>863                       | ω(Cδ1-H) (68)   |
| 772                       | 772                    | 869<br>860<br>853                | ω(Cδ1-H) (73); τ(Cγ-Cδ1) (11)<br>ω(Cε2-H) (41); ω(Cε3-H) (35); ω(Cε3-H) (18); τ(Cε2-Cε2) (11)<br>Ca-Ct (9); OCO (8)  | 825 (sh)<br>813 (w)<br>763 (sh) | 821 (w)<br>754 (s)     | 863<br>857<br>803                | ω(Cε3-H) (26); ω(Cε3-H) (22); ω(Cε3-H) (10); Cε2-Nε1-D (8)  |
| 766 (sh)                  |                        | 774                              | τ(Cε2-Cη) (29); τ(Cε3-Cε3) (24)<br>Cε2-Cε2' (10); Cδ2-Cε3 (9); Cδ2-Cγ (9)  | 881 (w)<br>754 (s)              | 860 (w)<br>756 (m)     | 777<br>768                       | ω(Cε3-H) (15); OCIO (12); Ca-Ct (11); Nt-Ca (11); Nd <sub>3</sub> <sup>+</sup> asym rock (10); W(O)••D(Nt) (10)                         |
| 758 (s)                   |                        | 754<br>578                       | ω(Cε2-H) (24); ω(Cη-H) (20); ω(Cε3-H) (39); ω(Cε3-H) (12)<br>ω(Nε1-H) (42); τ(Cε3-H) (18); ω(Cε2-Cη) (12)  | 708 (m)<br>578 (m)              | 708 (m)                | 755<br>751                       | τ(Cε2-Cη) (9); Cε2-Cε2' (8); ω(Cε3-H) (18); ω(Cε3-H) (10); τ(Cε2-Cη) (10)   |
| 710 (w)                   |                        | 758 (w)                          | ω(Cη-H) (11); ω(Cε2-H) (20); ω(Cε3-H) (39); ω(Cε3-H) (12)  |                                 |                        | 583                              | ω(Cε3-Cη) (69); ω(Cε3-H) (18); ω(Nε1-H) (16); τ(Cε3-H) (9)  |

<sup>a</sup>s, strong; m, medium; w, weak; sh, shoulder. Calcd.: Calculated wavenumbers from the lowest energy conformer (Figure 9, bottom) of tryptophan surrounded by six water molecules. See Table 4 for energy values. The angular bending modes of the tetrahedron located on the C<sub>β</sub> atom of the side chain are referred to as bending (-bend), wagging (-wag), twisting (-twist), and scissoring (-scissor).  $\vartheta$  and  $\tau$  designate an out-of-plane bending and a torsional internal coordinate, respectively. W = water. For atom numbering, see Figure 1.

**TABLE 4: Main Geometric and Energetic Features of Some Representative Lowest Energy Conformers of Amino Acids with Aromatic Side Chains<sup>a</sup>**

|                         | $\chi_1$ | $\chi_2$ | conformer | $E_e$       | $E_v$   | $E_{tot}$   | $\Delta E$ |
|-------------------------|----------|----------|-----------|-------------|---------|-------------|------------|
| Phe + 5H <sub>2</sub> O | -62.0    | 105.0    | $g^-g^+$  | -937.01830  | 198.751 | -936.70157  | 0.00       |
|                         | 55.9     | 76.6     | $g^+g^+$  | -937.01659  | 199.432 | -936.69877  | +1.67      |
|                         | -162.0   | 96.3     | $tg^+$    | -937.01548  | 198.925 | -936.69848  | +1.94      |
|                         | -68.2    | 103.4    | $g^-g^-$  | -937.01373  | 198.467 | -936.69745  | +2.58      |
| Tyr + 7H <sub>2</sub> O | 58.8     | -90.4    | $g^+g^-$  | -1165.12692 | 235.066 | -1164.75231 | 0.00       |
|                         | -59.2    | 102.6    | $g^-g^+$  | -1165.12144 | 233.340 | -1164.74958 | +1.71      |
|                         | -64.4    | -72.1    | $g^-g^-$  | -1165.11576 | 232.797 | -1164.74478 | +4.73      |
|                         | -172.7   | 87.2     | $tg^-$    | -1165.11656 | 233.558 | -1164.74433 | +5.01      |
| Trp + 6H <sub>2</sub> O | 51.3     | 84.4     | $g^+g^+$  | -1144.66150 | 233.014 | -1144.66150 | 0.00       |
|                         | 61.4     | -98.5    | $g^-g^-$  | -1145.03030 | 232.862 | -1144.65921 | +1.40      |
|                         | -58.0    | -87.1    | $g^-g^-$  | -1145.02907 | 232.302 | -1144.65887 | +1.60      |
|                         | -54.4    | 110.1    | $g^-g^+$  | -1145.02996 | 233.002 | -1144.65865 | +1.80      |

<sup>a</sup> See Figure 1 for the definition of  $\chi_1$  and  $\chi_2$  conformational angles.  $g^+$ ,  $g^-$ , and  $t$  refer to  $\chi_1$  and  $\chi_2$  angles.  $E_e$  (hartrees),  $E_v$  (kcal/mol) and  $E_{tot}$  (hartrees) correspond to electronic, zero-point vibrational and total energies, respectively.  $\Delta E$  (kcal/mol) is the energy difference with respect to the lowest energy conformer, whose energy is set to zero. See stereoviews of these conformers in Figures 7–9.

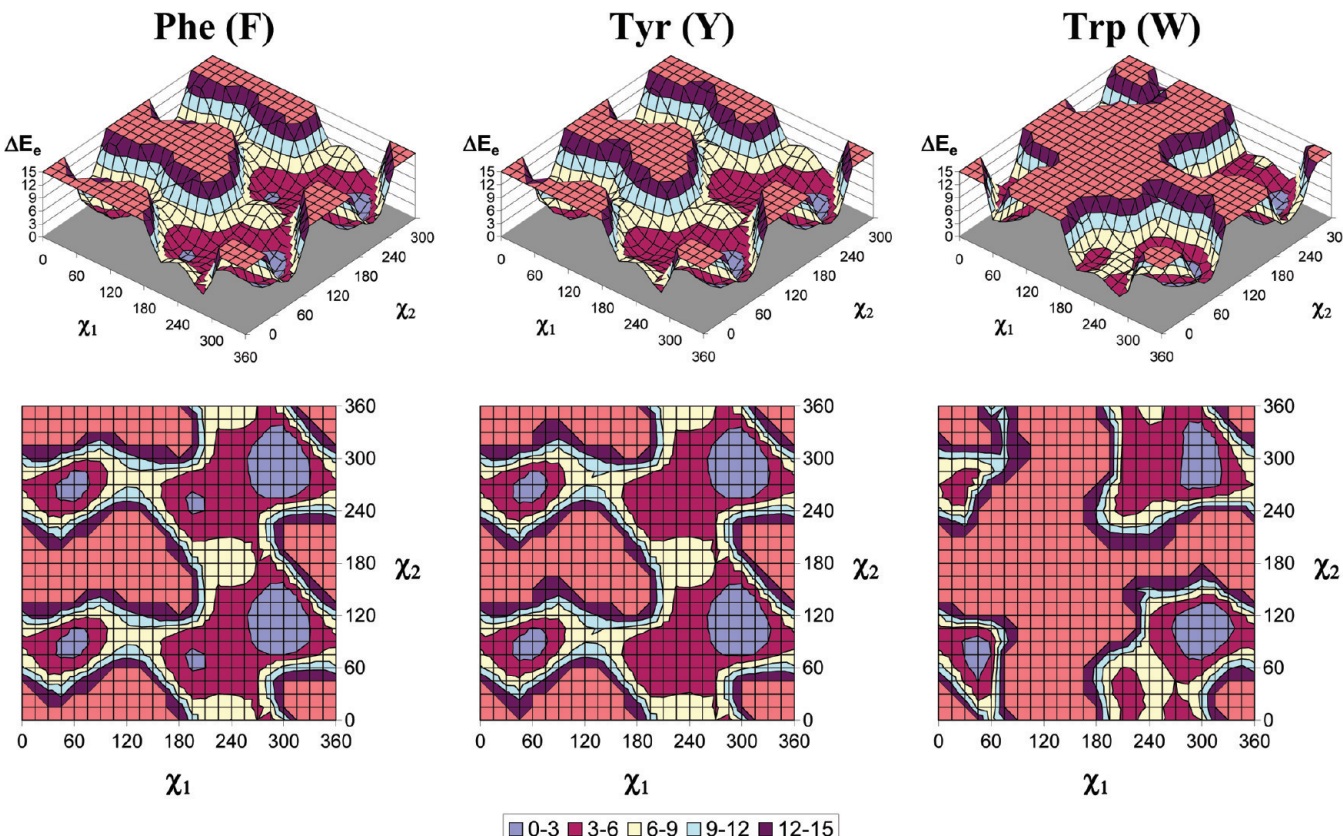


**Figure 6.** 3D (top row) and 2D (bottom row) representations of potential energy surfaces (PESs) showing the variation of electronic energy ( $E_e$ ) of the aromatic AAs embedded in a dielectric continuum, as a function of the conformational angles  $\chi_1$  and  $\chi_2$  (Figure 1). Note that the deepest valleys of these PESs are in blue color.

on the preparation of the samples used in SERS investigations,<sup>34</sup> and especially on their concentrations, is available. We should, however, mention that the presently reported Raman spectra provide a better resolution as well as a more important number of vibrational modes in the whole spectral region (1700–550 cm<sup>-1</sup>) in all the three AAs, especially in Tyr.

**III.2. Scan of the Energy Landscapes of the AAs Embedded in a Continuum Solvent.** In our recent publication devoted to histidine with neutral and positively charged side chains,<sup>32</sup> we have emphasized that the use of the potential energy surfaces (PESs) calculated in a continuum solvent environment can be considered as a first step in searching the most energetically favorable conformers in aqueous media. Figure 6 displays the PESs as a function of the side-chain conformational angles  $\chi_1$  and  $\chi_2$  (see Figure 1 and section II.2 for their definitions) within

a 15 kcal/mol energy range, beginning from the lowest energy (set to zero). We particularly focus our attention on the deepest valleys of these PESs (colored in blue, Figure 6) related to the most stable conformers. Phe, with its symmetric aromatic ring, present a blue valley in each of the six characteristic regions of the  $(\chi_1, \chi_2)$  map. However, among these energy minima, those located in the  $g^-g^+$  and  $g^-g^-$  regions are the most extended, whereas those in  $tg^+$  and  $tg^-$  are the narrowest ones (Figure 6, left). Here,  $t$ ,  $g^+$ , and  $g^-$  refer to trans, gauche<sup>+</sup>, and gauche<sup>-</sup> regions of these conformational angle. Tyr landscape presents only four blue valleys (Figure 6, center). This difference between Phe and Tyr landscapes arises evidently from the presence of extracyclic hydroxyl group in Tyr side chain. Finally, in Trp, the number of valleys is reduced to three, located in  $g^+g^+$  and  $g^-g^-$  and  $g^-g^+$  regions (Figure 6, right). In other words, upon

lowering the ring symmetry and/or increasing the ring size of the aromatic side chain ( $\text{Phe} \rightarrow \text{Tyr} \rightarrow \text{Trp}$ ), a more reduced number of regions in the  $(\chi_1, \chi_2)$  map can be accessed by the most energetically favorable conformers.

**III.3. Lowest Energy Conformers Optimized in the Presence of Explicit Hydration.** Conformers corresponding to the blue valleys, i.e., the deepest ones of the PESs presented in Figure 6 (see section III.2 for details), were selected as start points for our calculations with explicit hydration. Supramolecular assemblies containing a given AA surrounded with  $n$  water molecules were prepared for further geometry optimization. On the basis of our previous reports on the hydration analysis of a series of eight AAs,<sup>29–32</sup> we could conclude that a reasonable value for the number  $n$  might be equal to the H-bond donor and acceptor sites of a given AA. Through a discussion in the paper IV of this series,<sup>30</sup> based on the clusters including a leucine (Leu) surrounded by 5 and 12 water molecules, we could evidence the variation of geometrical and vibrational data upon increasing hydration number ( $n$ ). Especially, we have shown that the cluster Leu + 5H<sub>2</sub>O can be considered as a good compromise between the computation time and the geometrical and vibrational data expected from the theoretical calculations. Following this assumption, we have considered clusters with five, six, and seven water molecules for Phe, Trp, and Tyr, respectively. Each geometry optimization was followed by vibrational calculations. Accepted optimized conformers were those providing no imaginary frequency, thus confirming that they represent local energy minima of the landscapes. To get a better estimation of the relative energy of different conformers, we have considered their total energies  $E_{\text{tot}} = E_e + E_v$ .  $E_e$  and  $E_v$  are electronic and zero-point vibrational energies, respectively.  $E_v = 1/2\sum h\nu$ , where  $h$  is the Planck constant and  $\nu$  the frequency of one of the  $3N-6$  vibrational modes;  $N$  = total number of atoms. 43 conformers were accepted (see above) among 45 optimized in Phe, 179 conformers among 180 in Tyr, and 80 conformers among 84 in Trp. Obviously, we will not mention all accepted conformers, but only four for each AA (Table 4). Each lot of reported conformers includes the lowest energy conformer of the whole set of optimized conformers as well as three others corresponding to different conformational regions in  $(\chi_1, \chi_2)$  map, or to different rearrangements of water molecules. In Figure 7–9, the stereoviews of these characteristic conformers are displayed for Phe, Tyr, and Trp, respectively.

In the case of Phe + 5H<sub>2</sub>O cluster (Table 4, Figure 7), the first and last conformers in the energy scale, are  $g^-g^+$ . They are distinct one from the other by the location of water molecules. Beyond the hydration of the backbone COO<sup>-</sup> and NH<sub>3</sub><sup>+</sup> groups, one of the surrounding water molecules clearly interacts with the phenyl ring. The other two conformers,  $g^+g^+$  and  $tg^+$ , are both characterized by a short distance (<2.5 Å) separating one of the COO<sup>-</sup> oxygens from the extracyclic hydrogen connected to C<sub>δ</sub> atom. Note that  $tg^+$  conformer ( $\Delta E = +1.94$  kcal/mol) represents the most extended conformer with respect to the three others, corresponding to compact conformers surrounded by closed clusters of water molecules (Figure 7).

As far as the Tyr + 7H<sub>2</sub>O clusters are concerned (Table 4, Figure 8), it is to be noted that the two lowest energy conformers are  $g^+g^-$  and  $g^-g^+$ ; they are both compact, interacting with closed clusters of water molecules which hydrate their backbone and side chain polar groups. The other two conformers, i.e.,  $g^-g^-$  and  $tg^+$ , have higher relative energies, and disrupted clusters of water molecules, five of them interacting with the

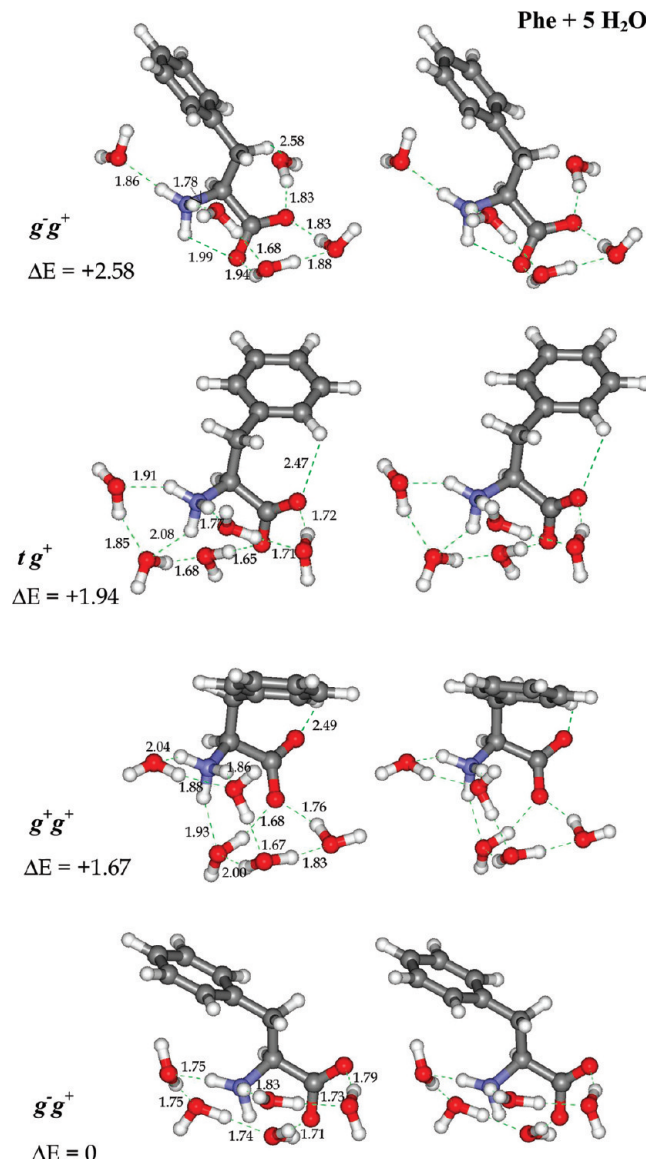


**Figure 7.** Stereoviews of the lowest energy conformers of phenylalanine surrounded by five water molecules. The conformations of each configuration, corresponding to the values of  $\chi_1$  and  $\chi_2$  angles (See Figure 1 for their definition), as well as its relative energy in kcal/mol, are reported on the left side of each view. See Table 4 and text for details. H-bonds are drawn with green broken lines and their lengths are reported in angströms.

backbone groups and the two others with the hydroxyl group of phenol ring.

Finally, in Trp + 6H<sub>2</sub>O (Table 4, Figure 9) the lowest energy conformers are  $g^+g^+$  and  $g^+g^-$  as in the case of Phe and Tyr (see above), and are compact structures, stabilized by interactions with closed clusters of water molecules. The other two conformers with higher relative energies, i.e.,  $g^-g^-$  and  $g^-g^+$  conformers, separate the bound water molecules into two groups, five of them interacting with the backbone and the last one with the N–H group of the aromatic side chain.

**III.4. Assignment of the Observed Vibrational Modes by Means of the Calculated Data Obtained from the Lowest Energy Conformers.** To assign the observed vibrational data (Figures 2–5), the lowest energy conformers of the explicitly hydrated AAs, i.e. those corresponding to  $\Delta E = 0$  in Table 4 (see also bottom graphics in Figures 7–9 and section III.3 for details) were used. Raw calculated wavenumbers, i.e., without

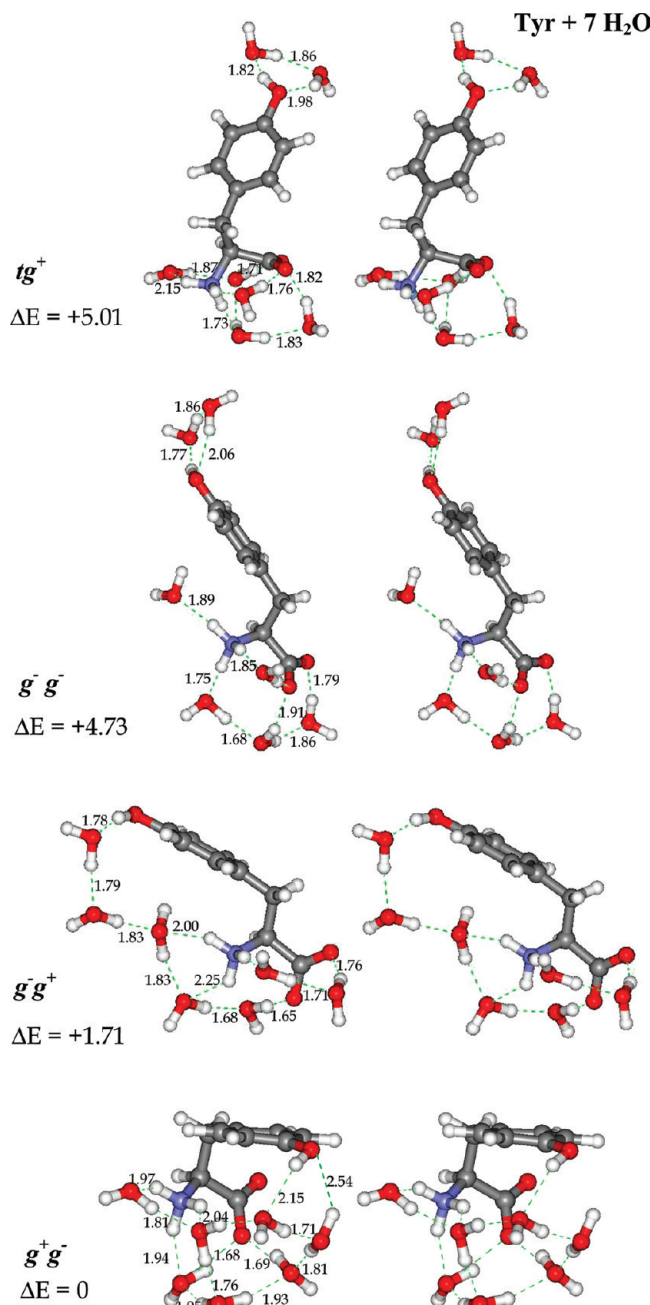


**Figure 8.** Stereoviews of the lowest energy conformers of tyrosine surrounded by seven water molecules. The conformations of each configuration, corresponding to the values of  $\chi_1$  and  $\chi_2$  angles (see Figure 1 for their definition), as well as its relative energy in kcal/mol, are reported on the left side of each view. See Table 4 and text for details. H-bonds are drawn with green broken lines and their lengths are reported in angströms.

the application of any scaling factor, were used for assigning the observed ones. This strategy leads to a better estimation of the inaccuracies related to the theoretical level, basis sets, as well as to the neglect of anharmonic effects. As it can be deduced from the comparisons reported in Tables 1–3, the average value of the scaling factor,  $r = \nu_{\text{exp}}/\nu_{\text{calc}}$  (where  $\nu_{\text{calc}}$  and  $\nu_{\text{exp}}$  are the calculated and observed wavenumbers of a given mode) is ca. 0.95, generally corresponding to a good theoretical level in the framework of harmonic approximation. Calculated vibrational modes were assigned on the basis of the PED (potential energy distribution) matrix

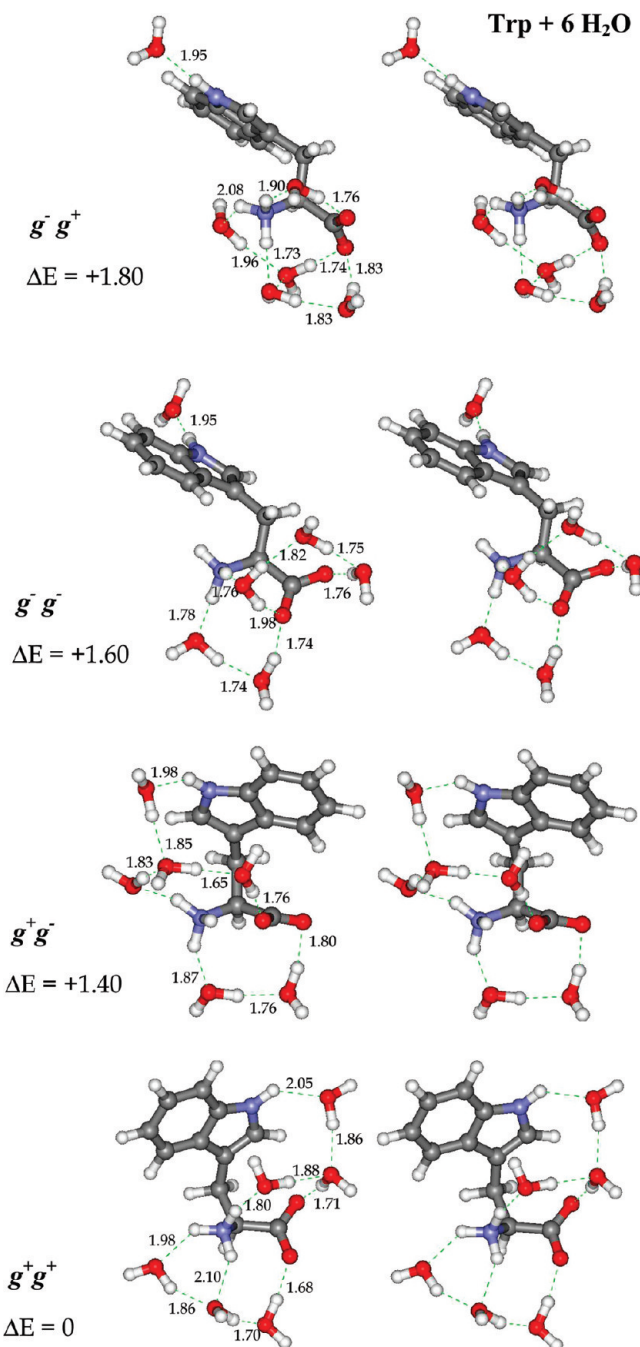


**Figure 9.** Stereoviews of the lowest energy conformers of tryptophan surrounded by six water molecules. The conformations of each configuration, corresponding to the values of  $\chi_1$  and  $\chi_2$  angles (see Figure 1 for their definition), as well as its relative energy in kcal/mol, are reported on the left side of each view. See Table 4 and text for details. H-bonds are drawn with green broken lines and their lengths are reported in angströms.

as expressed in terms of a combination of local symmetry and internal coordinates (Tables 1–3).

**Phenylalanine.** Raman spectra (Figure 2) are dominated by the intensity of the band at  $1004\text{ cm}^{-1}$ . Four other intense Raman bands exist at higher wavenumbers, i.e.,  $1032$ ,  $1207$ ,  $1586$ , and  $1606\text{ cm}^{-1}$ . All of these modes, being nonsensitive to deuteration, are assigned to the phenyl ring in-plane vibration modes (Table 1). In the low-wavenumber region, the ring-breathing mode at  $622\text{ cm}^{-1}$  is also assigned. Those modes sensitive to deuteration are generally of moderate intensity, mainly located

in the spectral region below  $1000\text{ cm}^{-1}$  in Raman spectra. The situation is different in FT-IR spectra, where the observed modes are perturbed by deuteration in the whole spectral range (Figure 3). In fact, Raman and FT-IR spectra do not reveal, with comparable intensities, the same vibrational modes. For instance,  $\text{NH}_3^+$  asymmetric bending as well as  $\text{COO}^-$  asymmetric stretching modes give rise to intense IR absorption bands, both sensitive to labile hydrogen deuteration because of the coupling between the terminal group vibrations through the AA backbone.

**Tyrosine.** Due to the presence of the hydroxyl group connected to the top of the side-chain aromatic ring (Figure 1), drastic changes appear in the vibrational spectra of this AA (Figure 4) in comparison with those of Phe (Figures 2 and 3). Especially, the effect of deuteration on ring in-plane modes, located above  $1000\text{ cm}^{-1}$ , is more important compared to that observed in Phe. The IR absorption band at  $1516\text{ cm}^{-1}$  (Figure 4) is assigned to an in-plane mode of aromatic ring (Table 2). Note also that, in Tyr, out-of-plane modes appear as more intense bands in the  $950\text{--}800\text{ cm}^{-1}$  spectral region of Raman spectra. Tyr ring-breathing mode is observed at  $643\text{ cm}^{-1}$  in Raman spectra, nonsensitive to deuteration on labile hydrogens (Table 2).

**Tryptophan.** Among the three analyzed AAs in this report, Trp provides the most complex vibrational spectra (Figure 5), because of the double-ring structure of its side chain (Figure 1). For example, intense Raman bands at 1621, 1579, 1012, and  $758\text{ cm}^{-1}$  are all assigned to the six-membered ring in-plane vibrations, whereas that at  $1552\text{ cm}^{-1}$  includes the vibrational motions of both five- and six-membered rings (Table 3). Slight wavenumber shifts are observed upon deuteration for some of the above-mentioned Raman bands. The intense Raman bands at  $880\text{ cm}^{-1}$  (medium intensity, vanishing in  $\text{D}_2\text{O}$ ) and at  $758\text{ cm}^{-1}$  (high intensity shifted to  $754\text{ cm}^{-1}$  in  $\text{D}_2\text{O}$ ) arise from the vibrational motions of the five- and six-membered rings. However, the breathing character (in-phase homothetical deformation of both rings) is more evident for the  $758\text{ cm}^{-1}$  Raman band. In contrast, IR absorption bands seem to mainly arise from the backbone vibrational motions (Table 3).

#### IV. Concluding Remarks

Our main conclusions can be summarized as follows:

(i) Despite the very low water solubility of tyrosine, we could finally record for the first time its Raman and FT-IR spectra in aqueous solutions (Figure 3). This was only made possible at a minimal concentration of  $2.3\text{ mM}$  ( $0.42\text{ mg/mL}$ ), just below the saturation condition of Tyr in aqueous solution.

(ii) Phe and Trp give rise to intense Raman bands (Figure 2 and 5), originating from the in-plane vibrations of aromatic side chains. These modes serve as useful vibrational markers in peptides and proteins. For instance, we can mention that the Raman spectra obtained from somatostatin, a 14-mer peptide hormone containing three Phe and one Trp residues in its chain, reported in paper V of this series,<sup>48</sup> are dominated by the intense bands arising from these AAs.

(iii) The common feature of all the AAs with an aromatic ring, i.e., His,<sup>32</sup> Phe, Tyr, and Trp, is their side-chain conformational flexibility thanks to the variation of  $\chi_1$  and  $\chi_2$  torsion angles (Figure 1). As evidenced by quantum mechanical calculations, their side chain can sweep a large space, rendering possible their interactions with the environment. Especially, water molecules, through their interactions with these AAs, seem

to facilitate the side-chain conformational transitions by lowering the energy barriers separating different conformers.

(iv) Theoretical calculations could also help us to better understand the interaction of water molecules with these AAs. Especially, solvent molecules can stabilize their interactions by pointing one of their hydrogens toward the aromatic ring; see, for instance, graphic representations of  $\text{g}^-\text{g}^+$  conformers in Phe +  $5\text{H}_2\text{O}$  (Figure 7),  $\text{g}^-\text{g}^-$  and  $\text{g}^-\text{g}^+$  conformers in Tyr +  $7\text{H}_2\text{O}$  (Figure 8), as well as  $\text{g}^+\text{g}^-$  conformer in Trp +  $6\text{H}_2\text{O}$  (Figure 9). This special manner of interaction of a proton with an aromatic ring seems to be interesting and leads us to emphasize, for instance, the previously published results on helical stabilization observed upon lowering pH in the peptide chains containing Trp and His residues located at *i* and *i* + 4 positions, respectively.<sup>49</sup> In fact, by decreasing pH toward acidic values, where His ring is protonated on both of its nitrogens,<sup>32</sup> one could expect a better interaction of the protonated His with the Trp aromatic ring found in its proximity due to the helical conformation of a peptide chain.

**Acknowledgment.** This work was granted access to the HPC resources of CINES (Montpellier, France) under the allocation 2010-c2010075065 made by GENCI (Grand Equipement National de Calcul Intensif). Numerical calculations on geometrical and vibrational properties of aromatic amino acids were realized on the Jade (SGI) supercomputing network installed in CINES.

**Supporting Information Available:** Vibrational spectra of tyrosine in solid and heterogeneous phases (Figure S1), as well as atomic Cartesian coordinates of the 12 low-energy conformers displayed in Figures 7–9 (see also Table 4), obtained by full geometry optimization in the presence of explicit solvent, are provided. This material is available free of charge via the Internet at <http://pubs.acs.org>.

#### References and Notes

- Fürst, P.; Stehle, P. *J. Nutr.* **2004**, *134*, 1558S–1565S.
- Reeds, P. *J. Nutr.* **2000**, *130*, 1835S–1840S.
- Young, V. R. *J. Nutr.* **1994**, *124*, 1517S–1523S.
- Schulz, G. E.; Schrimmer, R. H. *Principles of Protein Structure*; Cantor, R. H., Ed.; Springer-Verlag: New York, 1990.
- Gonzalez, J.; Willis, M. S. *Lab. Med.* **2010**, *41*, 118–119.
- Ikeda, M. *Adv. Biochem. Eng. Biotechnol.* **2002**, *79*, 1–35.
- Redgrave, P.; Gurney, K. *Nat. Rev. Neurosci.* **2006**, *7*, 967–975.
- Ben-Jonathan, N.; Hnasko, R. *Endocr. Rev.* **2001**, *22*, 724–763.
- Manning, G.; Whyte, D. B.; Martinez, R.; Hunter, T.; Sudarsanam, S. *Science* **2002**, *298*, 1912–1934.
- Wang, J. C. *Annu. Rev. Biochem.* **1985**, *54*, 665–697.
- Radwanski, E. R.; Last, R. L. *Plant. Cell.* **1995**, *7*, 921–34.
- Fernstrom, J. D. *Physiol. Rev.* **1983**, *63*, 484–546.
- Schaechter, J. D.; Wurtman, R. J. *Brain Res.* **1990**, *532*, 203–210.
- Gollnick, P.; Babitzke, P.; Antson, A.; Yanofsky, C. *Annu. Rev. Genet.* **2005**, *39*, 47–68.
- Matthews, B. W.; Sigler, P. B.; Henderson, R.; Blow, D. M. *Nature* **1967**, *214*, 652–656.
- Blow, D. M.; Birktoft, J. J.; Hartley, B. S. *Nature* **1969**, *221*, 337–340.
- van Grondelle, W.; López Iglesias, C.; Coll, E.; Artzner, F.; Paternostre, M.; Lacombe, F.; Cardus, M.; Martinez, G.; Montes, M.; Cherif-Cheikh, R.; Valéry, C. *J. Struct. Biol.* **2007**, *160*, 211–223.
- Valéry, C.; Pouget, E.; Pandit, A.; Verbavatz, J. M.; Bordes, L.; Boisdé, I.; Cherif-Cheikh, R.; Artzner, F.; Paternostre, M. *Biophys. J.* **2008**, *94*, 1782–1795.
- McGaughey, G. B.; Gagne, M.; Rappe, A. K. *J. Biol. Chem.* **1998**, *273*, 15458–15463.
- Sal-Man, N.; Gerber, D.; Bloch, I.; Shai, Y. *J. Biol. Chem.* **2007**, *282*, 19753–19761.
- Principles of Fluorescence Spectroscopy*, 2nd ed.; Lakowicz, J. R., Ed.; Kluwer Academic/Plenum Publishers: New York, 1999.
- New Trends in Fluorescence Spectroscopy*; Valeur, B., Bronchon, J. C., Eds.; Springer-Verlag: Berlin, 2001.
- Denk, W.; Strickler, J.; Webb, W. *Science* **1990**, *248*, 73–76.

- (24) Denk, W.; Svoboda, K. *Neuron* **1997**, *18*, 351–357.  
(25) Helmchen, F.; Denk, W. *Nat. Methods* **2005**, *2*, 932–940.  
(26) Dunker, A. K.; Williams, R. W.; Peticolas, W. L. *J. Biol. Chem.* **1979**, *254*, 6444–6448.  
(27) Aubrey, K. L.; Thomas, G. J., Jr. *Biophys. J.* **1991**, *60*, 1337–1349.  
(28) Barth, A. *Prog. Biophys. Mol. Biol.* **2000**, *74*, 141–173.  
(29) Derbel, N.; Hernández, B.; Pflüger, F.; Liquier, J.; Geinguenaud, F.; Jaïdane, N.; Ben Lakhdar, Z.; Ghomi, M. *J. Phys. Chem. B* **2007**, *111*, 1470–1477.  
(30) Hernández, B.; Pflüger, F.; Nsangou, M.; Ghomi, M. *J. Phys. Chem. B* **2009**, *113*, 3169–3178.  
(31) Hernández, B.; Pflüger, F.; Derbel, N.; De Coninck, J.; Ghomi, M. *J. Phys. Chem. B* **2010**, *114*, 1077–1088.  
(32) Pflüger, F.; Hernández, B.; Ghomi, M. *J. Phys. Chem. B* **2010**, *114*, 9072–9083.  
(33) Wolpert, M.; Hellwig, P. *Spectrochim. Acta A* **2006**, *64*, 987–1001.  
(34) Stewart, S.; Fredericks, P. M. *Spectrochim. Acta A* **1999**, *55*, 1641–1660.  
(35) Jákli, I.; Perczel, A.; Farkasa, Ö.; Hollósi, M.; Csizmadia, I. G. *J. Mol. Struct. (THEOCHEM)* **1998**, *455*, 303–314.  
(36) Huang, Z.; Yu, W.; Lin, Z. *J. Mol. Struct. (THEOCHEM)* **2006**, *758*, 195–202.  
(37) Rodziewicz, P.; Doltsinic, N. L. *ChemPhysChem* **2007**, *8*, 1959–1968.  
(38) Lakard, B. *J. Mol. Struct. (THEOCHEM)* **2004**, *681*, 183–189.  
(39) Zhang, M.; Huang, Z.; Lin, Z. *J. Chem. Phys.* **2005**, *122*, 134313–134319.  
(40) Sobolewski, A. L.; Shemesh, D.; Domcke, W. *J. Chem. Phys. A* **2009**, *113*, 542–550.  
(41) Gao, B.; Wyttenbach, T.; Bowers, M. T. *J. Am. Chem. Soc.* **2009**, *131*, 4695–4701.  
(42) Kohn, W.; Sham, L. *J. Phys. Rev.* **1965**, *140*, A1133–A1138.  
(43) Becke, A. D. *J. Chem. Phys.* **1993**, *98*, 5648–5652.  
(44) Lee, C.; Yang, W.; Parr, R. G. *Phys. Rev. B* **1988**, *37*, 785–789.  
(45) Frisch, M. J.; Trucks, G. W.; Schlegel, H. B.; Scuseria, G. E.; Robb, M. A.; Cheeseman, J. R.; Montgomery Jr., J. A.; Vreven, T.; Kudin, K. N.; Burant, J. C.; Millam, J. M.; Iyengar, S. S.; Tomasi, J.; Barone, V.; Mennucci, B.; Cossi, M.; Scalmani, G.; Rega, N.; Petersson, G. A.; Nakatsuji, H.; Hada, M.; Ehara, M.; Toyota, K.; Fukuda, R.; Hasegawa, J.; Ishida, M.; Nakajima, T.; Honda, Y.; Kitao, O.; Nakai, H.; Klene, M.; Li, X.; Knox, J. E.; Hratchian, H. P.; Cross, J. B.; Bakken, V.; Adamo, C.; Jaramillo, J.; Gomperts, R.; Stratmann, R. E.; Yazyev, O.; Austin, A. J.; Cammi, R.; Pomelli, C.; Ochterski, J. W.; Ayala, P. Y.; Morokuma, K.; Voth, G. A.; Salvador, P.; Dannenberg, J. J.; Zakrzewski, V. G.; Dapprich, S.; Daniels, A. D.; Strain, M. C.; Farkas, O.; Malick, D. K.; Rabuck, A. D.; Raghavachari, K.; Foresman, J. B.; Ortiz, J. V.; Cui, Q.; Baboul, A. G.; Clifford, S.; Cioslowski, J.; Stefanov, B. B.; Liu, G.; Liashenko, A.; Piskorz, P.; Komaromi, I.; Martin, R. L.; Fox, D. J.; Keith, T.; Al-Laham, M. A.; Peng, C. Y.; Nanayakkara, A.; Challacombe, M.; Gill, P. M. W.; Johnson, B.; Chen, W.; Wong, M. W.; Gonzalez, C.; Pople, J. A. *Gaussian 03, Revision C.02*; Gaussian, Inc.: Wallingford, CT, 2004.  
(46) Barone, V.; Cossi, M. *J. Phys. Chem. A* **1998**, *102*, 1995–2001.  
(47) Cossi, M.; Rega, G.; Scalmani, G.; Barone, V. *J. Comput. Chem.* **2003**, *24*, 669–681.  
(48) Hernández, B.; Carelli, C.; Coic, Y. M.; De Coninck, J.; Ghomi, M. *J. Phys. Chem. B* **2009**, *113*, 12796–12803.  
(49) Fernández-Recio, J.; Vázquez, A.; Civera, C.; Sevilla, P.; Sancho, J. *J. Mol. Biol.* **1997**, *267*, 184–197.

JP106786J